CDF/ANAL/ELECTROWEAK/CDFR/6535
Version 1.5
2004/03/08

Measurement of the $\sigma(p\bar{p} \to W) \times BF(W \to e\nu)$ in the Plug Region Using Combined Calorimetric and Forward Tracking Information

G. Chiarelli, I. Fedorko, S. Leone, A. Sidoti

University of Pisa and INFN Pisa

Abstract

We present a measurement of the $\sigma(p\overline{p} \to W) \times BF(W \to e\nu)$ at $\sqrt{s}$ 1.96 TeV in the plug region for $|\eta|$ <2.8 using combined calorimetric and tracking information. After analyzing 64 pb^{-1} of data collected in CDF Run II we measure a cross section of 2.874 ±0.034(stat)± 0.167(syst) ± 0.172 (lum.) nb. The result is in agreement with previous CDF measurements in the central region and with theoretical estimates.

1 Introduction

We present a measurement of the W($\to e\nu$) cross section in the plug region, using combined calorimetric and tracking information. The main aim of this work is to exploit a known physics process, to optimize reconstruction code and strategies for tracking in the forward region. The measurement of a cross section allows to check expectation for performances mostly -so far- based on Monte Carlo. While the strategy is just the same as for the central region, the hardware and software

tools are quite different. Plug EM calorimeter takes the role of the Central EM and (mostly) Standalone Silicon Tracking replaces the COT-based tracks of the central region. Besides trigger, tracking efficiencies are to be established. At the same time, as the W cross section is a (relatively) well known number, we plan to use this measurement as a benchmark to throughly check tracking reconstruction and Monte Carlo in the $|\eta| > 1$ region. In this analysis we use 3D tracks only, reconstructed *without* using any calorimetric information. Therefore the PHOENIX algorithm (which identifies electron candidates by matching EM clusters in the plug with 2D silicon tracks seeded by the cluster itself) is not used.

The ingredients needed for this analysis are those contained in the basic equation: $\sigma = (N_{ev} - B)/(\epsilon \times L)$, where N_{ev} is the number of selected events, B is the remaining background, L is the integrated luminosity and ϵ is the product of kinematical, geometrical, trigger and reconstruction efficiencies.

2 Data Sample and Data Reduction

The data set we use corresponds to runs between 141544 and 156847 taken from February 2002 until the January 2003 shutdown. Only good runs (according to [1]) are selected. We apply a number of selection criteria to strip events out of Production dataset BPEL08 and run them through reconstruction code (Offline version 4.10.4). 12 pb^{-1} of data corresponding to runs between 152595 and 154012 were taken from dataset BPEL09 as the corresponding files in dataset BPEL08 were reconstructed with wrong alignment constants (and therefore removed in our sample) [2]. For the measurement itself we use events collected by trigger path PEM_MET. All known plug energy and alignment corrections were applied ([3], [4]). In order to measure efficiencies, check energy scale etc., other trigger paths within the same dataset were also used.

The following criteria are applied in cascade:

- Primary Z vertex $|Z_{vtx}|$ <60 cm;

- EM cluster belongs to PLUG with 1.1< $|\eta|$ <2.8;
- calorimetric EM cluster with $E_T > 20$ GeV;
- Missing Transverse Energy (MET)> 20 GeV.

All quantities are corrected for primary vertex information. EM energy is also corrected for time-dependent effects. After those selection criteria we are left with 243650 candidate events. Table 1 summarizes the number of events passing each cut.

requirement	N.of events	East	West
Trigger	1.09734×10^6	N/A	N/A
Nprimary => 1	976373	N/A	N/A
$\|P_{VZ}\| < 60$ cm	762572	N/A	N/A
At least one Em object	761831	523044	501294
plug region and 1.1< $\|\eta\|$ < 2.8	716279	397480	393653
$E_T > 20$ GeV	691829	351248	349682
$MET > 20$ GeV	243650	117236	128068
Isorel< 0.1, Had/Em< 0.05	90265	43098	47167
Matching track	18181	9357	8824
$0.5 < E/p < 2$	10461	5409	5052

Table 1: Events of the Data sample passing the various cuts.

Figure 1 shows the MET vs transverse energy of the electron candidates. Electrons from W decay cluster along the diagonal, but a large background is clearly visible.

Two ID cuts are applied to electron candidates:

- IsoRel< 0.1;
- Had/Em < 0.05.

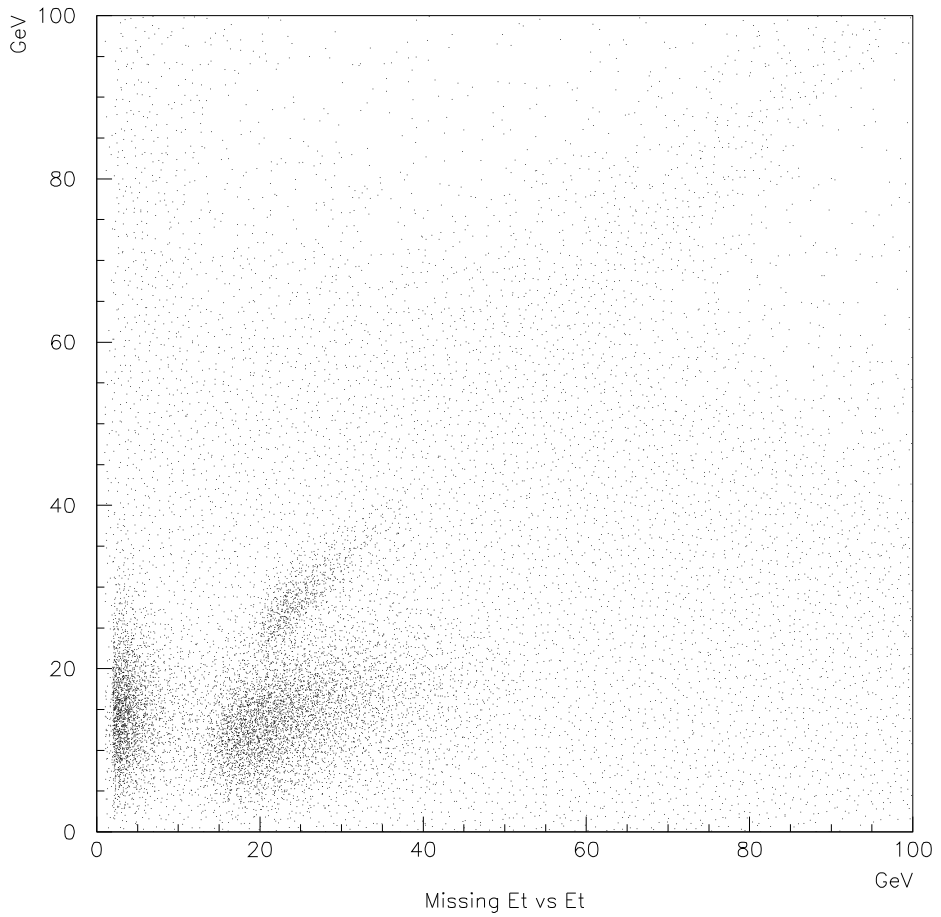

Figure 1: *MET vs transverse energy of candidate electrons.*

At this stage of data reduction, 90265 (43098 on the East side) events pass our requirements. We compare kinematical variables in data to expectation from $W \to e\nu$ Monte Carlo. In the following plots we show data (dots) superimposed to MC (in yellow) for several kinematical quantities. To ease shape comparisons, histograms were normalized to one. Figure 2 and figure 3 show φ and η of electron candidates. Figure 4 the E_T of the electron (as E_T of the electron we use "PEM

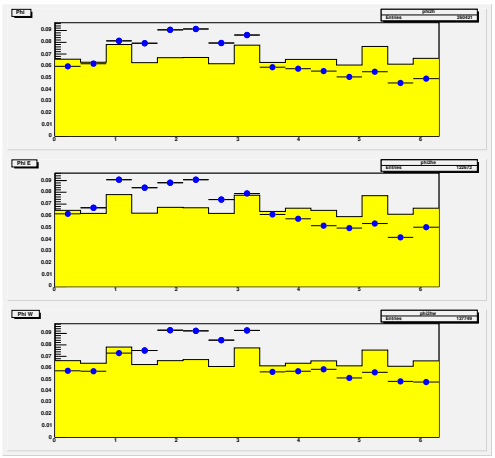

Figure 2: *φ distribution for electron candidates in W sample after calorimetric selection. Data (dots) superimposed to MC(yellow histogram). Top plot: East and West combined, center: East side, bottom: West side.*

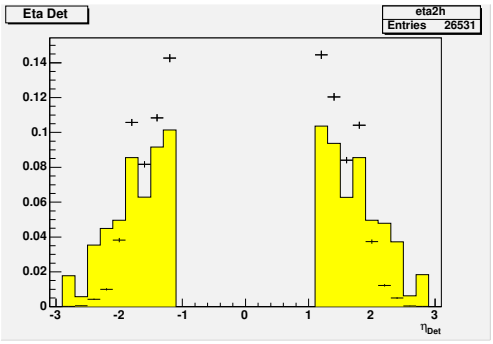

Figure 3: *η distribution for electron candidates in W sample after calorimetric selection. Data (dots) superimposed to MC(yellow histogram).*

3x3" corrected for primary vertex position, time dependent effects, face effects and energy measured by the PPR [5]) while figure 5 shows the MET distribution. Finally transverse mass distribution M_T is shown in figure 6.

By looking at those plots, it is clear that background is largely dominating our data. No Jacobian peak is visible in the M_T distribution and signal in MET distribution is swamped by background.

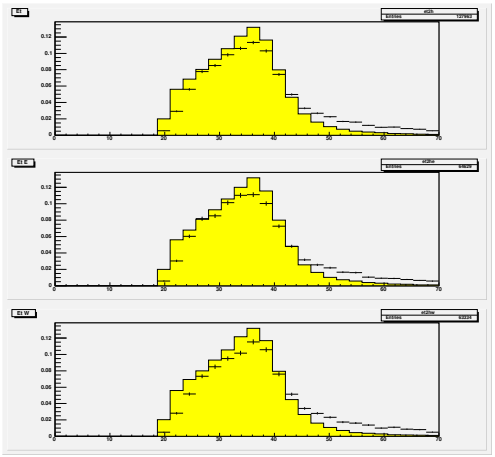

Figure 4: *E_T distribution for electron candidates in W sample after calorimetric selection. Data (dots) superimposed to MC(yellow histogram). Top plot: East and West combined, center: East side, bottom: West side.*

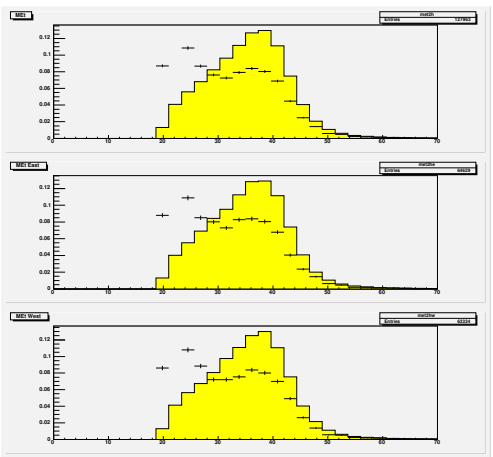

Figure 5: *MET distribution in W candidate events after calorimetric selection. Data (dots) superimposed to MC(yellow histogram). Top plot: East and West combined, center: East side, bottom: West side.*

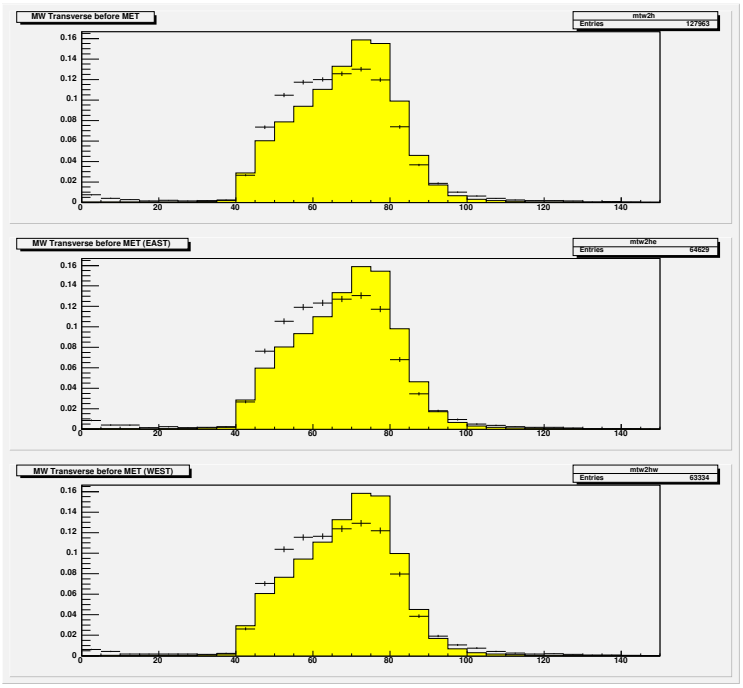

Figure 6: *M_T for W candidate events after calorimetric selection. Data (dots) superimposed to MC(yellow histogram). Top: East and West, center: East side, bottom: West side.*

2.1 Use of Forward Tracking

In order to clean up our data sample, we require events to have at least one 3D track with P_T >1 GeV/c, pointing to the EM cluster within a cone radius of ΔR <0.4 and extrapolating to the PES to better than 3 cm in the X and Y coordinates. Cut was optimized by using the $Z \rightarrow ee$ sample (see section below for a description of the sample). Figure 7 shows the distribution of ΔX, ΔY (extrapolated track- PES

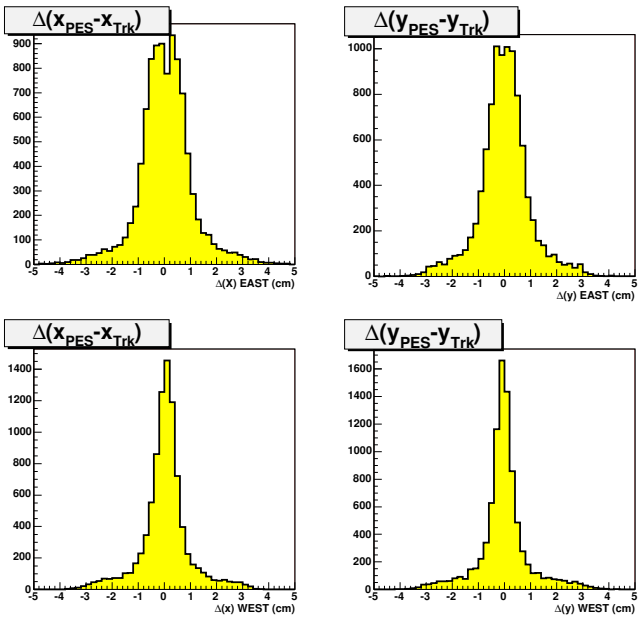

Figure 7: *Residuals (X, Y) for tracks extrapolated to PES for electron candidates in W sample. Top plots: East side, bottom: West side.*

measured coordinate) for West and East candidates separately. PES measurements are corrected for all known effects [5, 3]. Figure 8 shows the same distribution for the plug leg of $Z \rightarrow ee$ candidates.

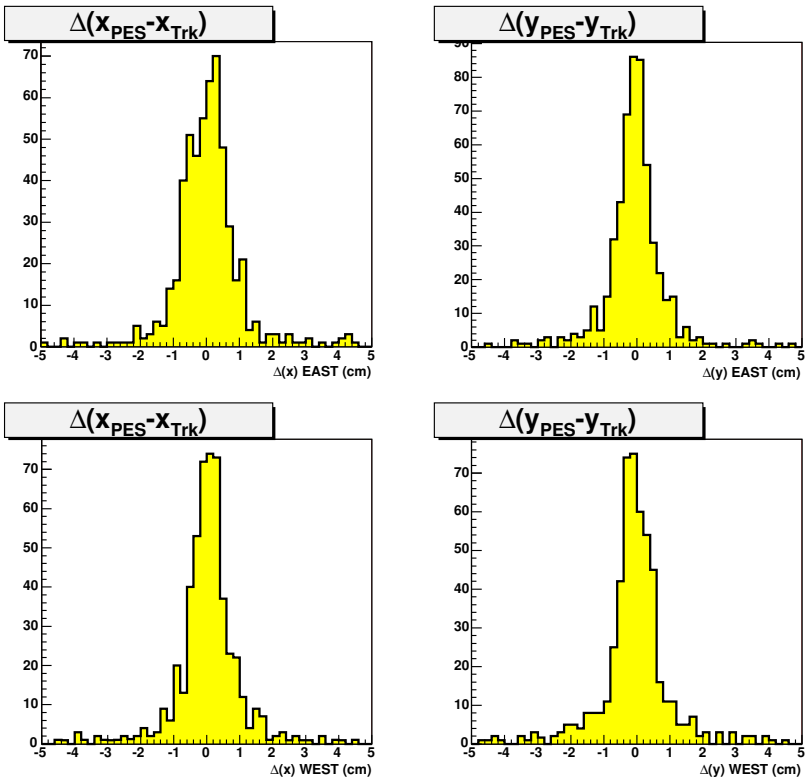

Figure 8: *Residuals (X, Y) for tracks extrapolated to PES in $Z \rightarrow ee$ sample. Top plots: East side, bottom: West side.*

Figure 9 shows the distribution of tracking algorithms contributing to our sample. Major role is played by Outside-In and SiliconStandalone.

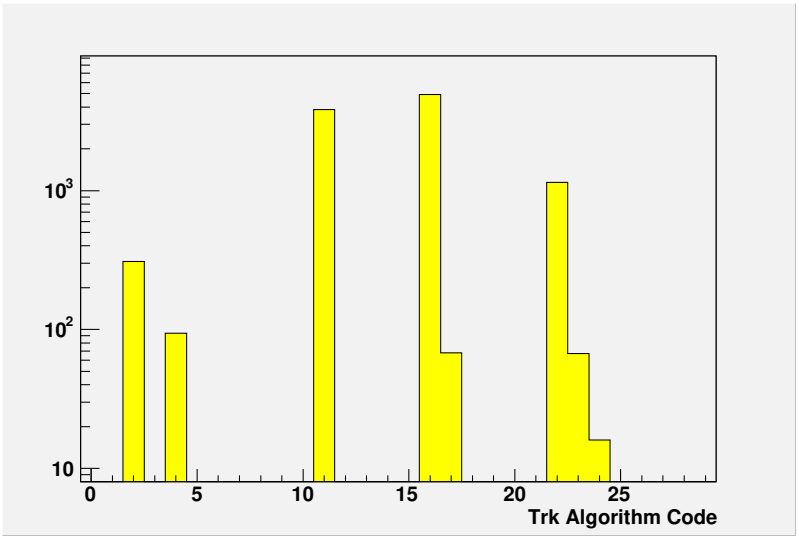

Figure 9: *Forward tracks. Contribution to the final sample divided by tracking algorithm. Outside-in is algorithm with code 11, Silicon Standalone(SiSA) is algorithm with code 16.*

Last criteria applied is an E/p matching. In figure 10 we show data and Monte Carlo comparison before applying the final cut on this quantity. An excess at large E/p, indication of missing material in Monte Carlo, is visible. We require 0.5< E/p <2. 10461 candidate events pass this final cut. 5409 events are found in the EAST plug, 5052 in the WEST. Scatter plot of MET vs E_T (figure 11) shows the correlation characteristic of the W signal.

Figure 12 shows the primary vertex distribution for candidate events. Data and MC are normalized to one and superimposed. There is a clear indication, mostly visible in the distributions relative to EAST and WEST regions, of the limited geometrical acceptance of our selection which is sculpting the Z vertex distribution. The agreement, however, is excellent showing that Monte Carlo is well reproducing

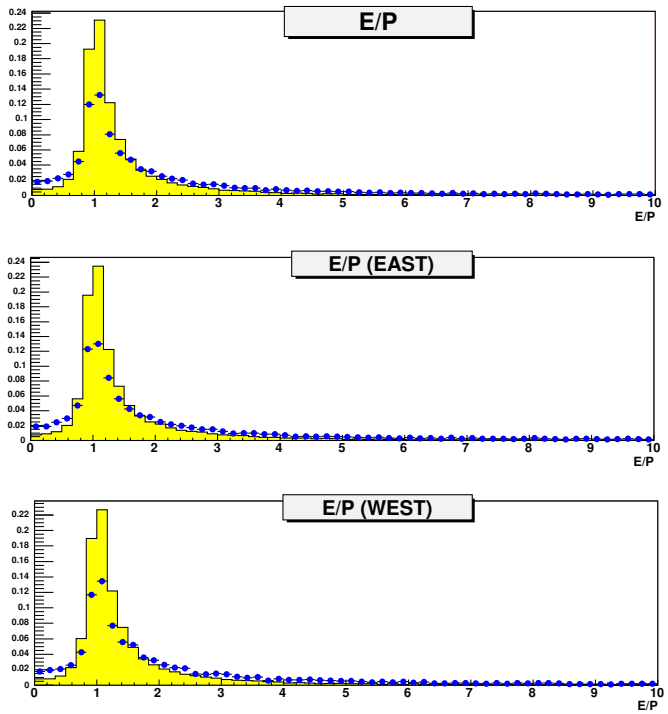

Figure 10: *E/p distribution for electron candidates before E/p cut.*

the shape of the signal.

Comparison of several kinematical quantities after selection is provided in the following figures, where MC is the histogram and dots are data.

Distribution for electron candidates φ and detector η are shown in figure 13 and figure 14. Figure 15 shows E_T distribution, figure 16 the MET distribution.

Finally comparison of data and MC for M_T is given in figure 17.

Although at this stage no background has been subtracted, histograms support a qualitative statement that, thanks to track matching, data have been cleaned up. The jacobian peak is visible in the M_T distribution of candidate events, and the MET and E_T distributions in fig. 16 and 15 exhibit the characteristic shape of the debris of a two-body decay.

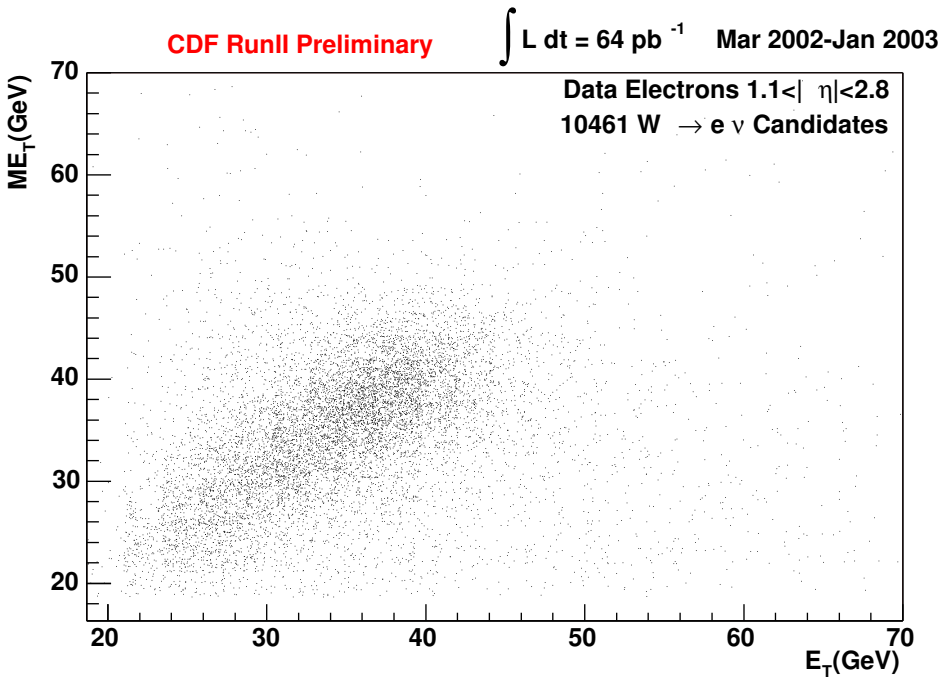

Figure 11: *MET vs E_T for W candidates events.*

3 $Z \to ee$ Sample

Z events with one of the two legs being reconstructed in the plug, constitute a good control sample. We select events with a *tight* central electron and a *loose* plug candidate according to selection criteria studied by A. Robson et al. for the analysis of the $\sigma \cdot Br(Z^0 \to e^+e^-)$ [6]. Figure 18 shows M_{ee} in our data sample compared to Monte Carlo expectations. The results returned by fitting the distribution are in agreement with MC and close to the PDG value. In the following, for our studies, we use events contained in up to $\pm 15\ GeV/c^2$ around the mass peak of the Z.

Figure 20 and 19 show the φ and η distributions for the plug leg of Z (CP) electron candidates. A good agreement between data and MC is visible.

Figure 21 shows the E_T distribution for the same electron candidates. Again

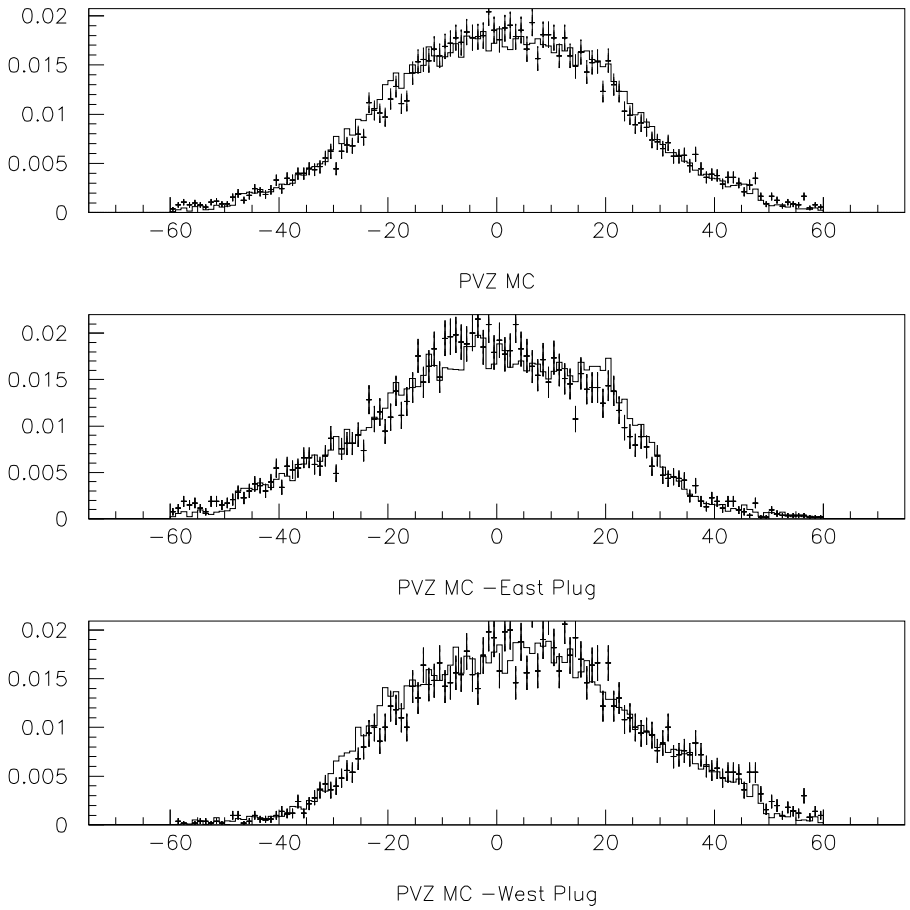

Figure 12: *Primary vertex distribution for W candidate events. Data (dots) and MC superimposed. Top: East and West, center: East side, bottom: West side.*

agreement between data and MC is good.

Efficiency of Had/Em and relative isolation cuts are measured using this sample (see below). After requiring the match of an EM cluster in the plug with a reconstructed 3D track, we use this sample of $Z \to ee$ CP events to study the tracking reconstruction efficiency for forward electron and to compare data and MC.

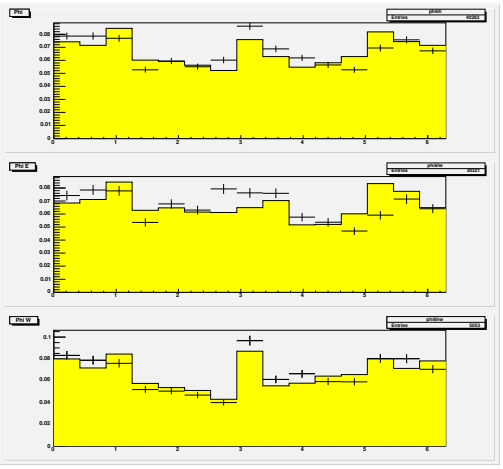

Figure 13: *φ of electron candidates. Data (dots) and MC superimposed. Top: East and West, center: East side, bottom: West side.*

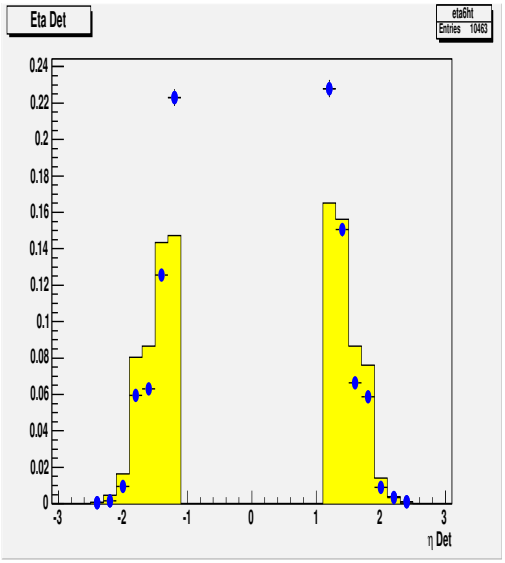

Figure 14: *Detector η distribution for electron candidates. Data (dots) and MC superimposed.*

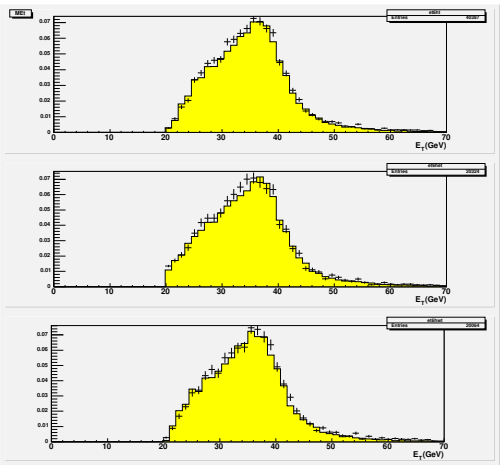

Figure 15: *E_T of electron candidates. Data (dots) and MC superimposed. Top: East and West, center: East side, bottom: West side*

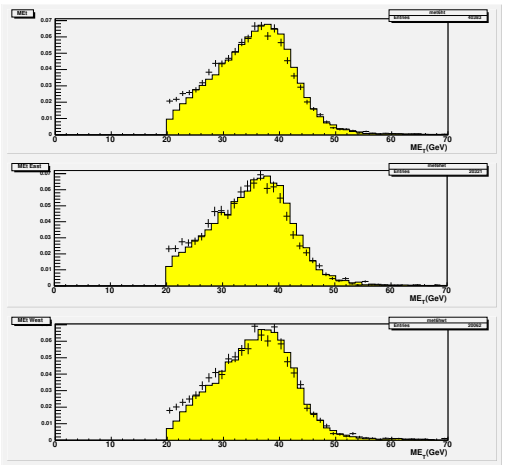

Figure 16: *MET in selected events. Data (dots) and MC superimposed. Top: East and West, center: East side, bottom: West side.*

4 Kinematical and geometrical acceptances

To estimate kinematical and geometrical acceptances we used realistic Monte Carlo samples. 430,500 $W \to e\nu$ events generated with Pythia 6.203 (CTQ5L) of release

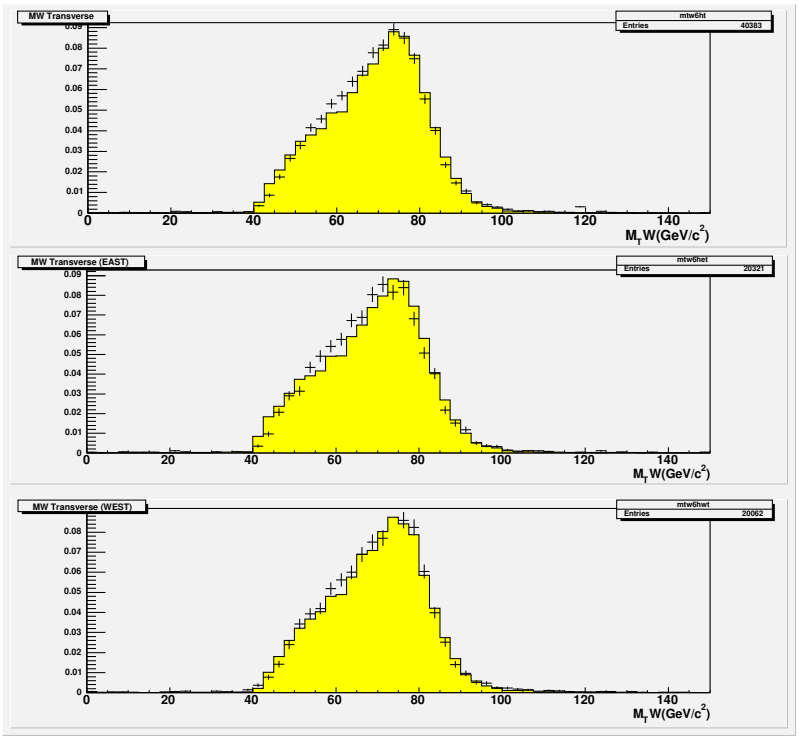

Figure 17: *Transverse mass for W candidates. Data (dots) and MC superimposed. Top: East and West, center: East side, bottom: West side.*

4.9.1 and reconstructed using 4.11.1.

The Monte Carlo is tuned to provide the best possible match with data in W boson p_T distribution and in E/p distribution, with an appropriate description of the material [9].

E_T is tuned to data using a sample of $Z \to ee$ CP events and therefore E_T was scaled up by 2.5% and smeared by 2.7% [6].

The model of energy deposition in calorimeter is tuned by matching data and MC for recoil energy $\vec{U}$(deposited energy in calorimeter without energy associated with the lepton, i.e. $\vec{U} = -M\vec{E}T - \vec{E}_T^e$).

Geometrical efficiency is defined as the ratio of events passing our cuts divided

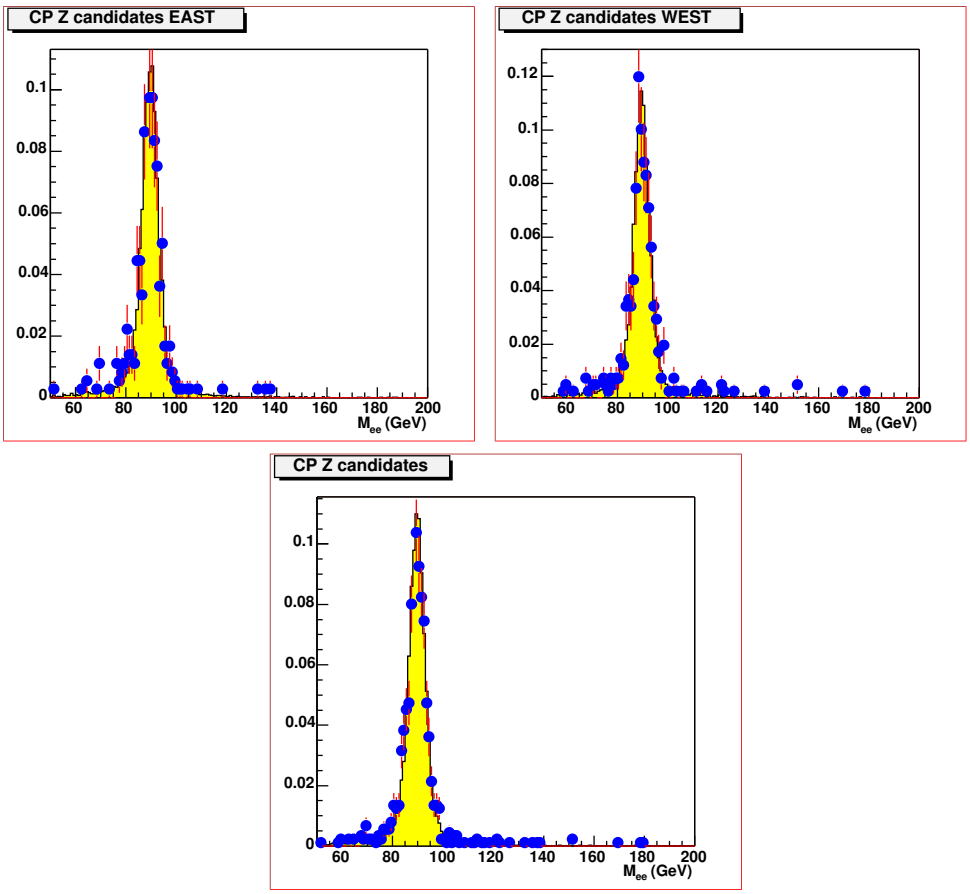

Figure 18: *Invariant mass for $Z \to ee$ CP candidates. Data (dots) superimposed to MC (yellow).*

by the number of events with a generated vertex with $|Z_{vtx}| < 60$ cm.

In table 2 we list the number of Montecarlo events passing the various cuts. The total geometrical efficiency is 0.3112 ± 0.00072 (stat. only).

4.1 Systematic uncertainty on acceptance

We calculated the systematic uncertainty on acceptance due to the following effects:

- Energy Scale and Resolution;

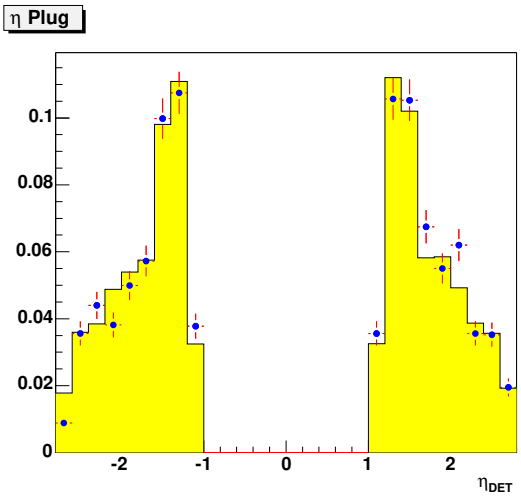

Figure 19: *Detector η distribution for $Z \to ee$ CP candidates. Data (dots) and MC superimposed.*

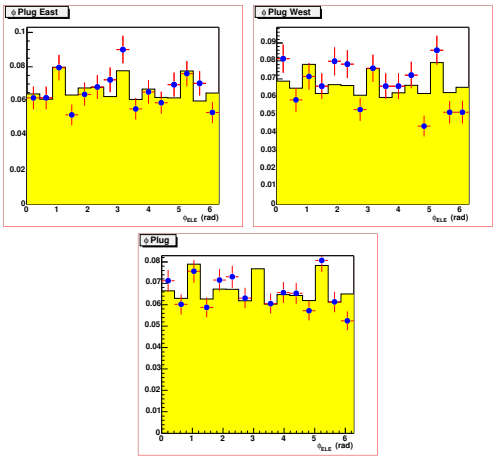

Figure 20: *φ distribution of plug leg in CP Z candidates. Data (dots) and MC superimposed.*

requirement	N.of generated events
Generated events	430500
generated with $\lvert Z_{vtx}\rvert < 60$	416315
at least one EM cluster	399348
plug region and $1.1 < \lvert\eta\rvert < 2.8$	194922
$E_T > 20$ GeV	139219
$MET > 20$ GeV	129551

Table 2: Events of the MC $W \to e\nu$ sample passing the various cuts.

- P_T of W;
- Extra Material;
- Recoil Energy Modeling;
- PDF Uncertainty.

The uncertainty on the electron E_T cut was evaluated by varying the plug EM energy scale and energy resolution by $\pm 0.6\%$ and $\pm 1.1\%$, corresponding to $\pm 3\sigma$

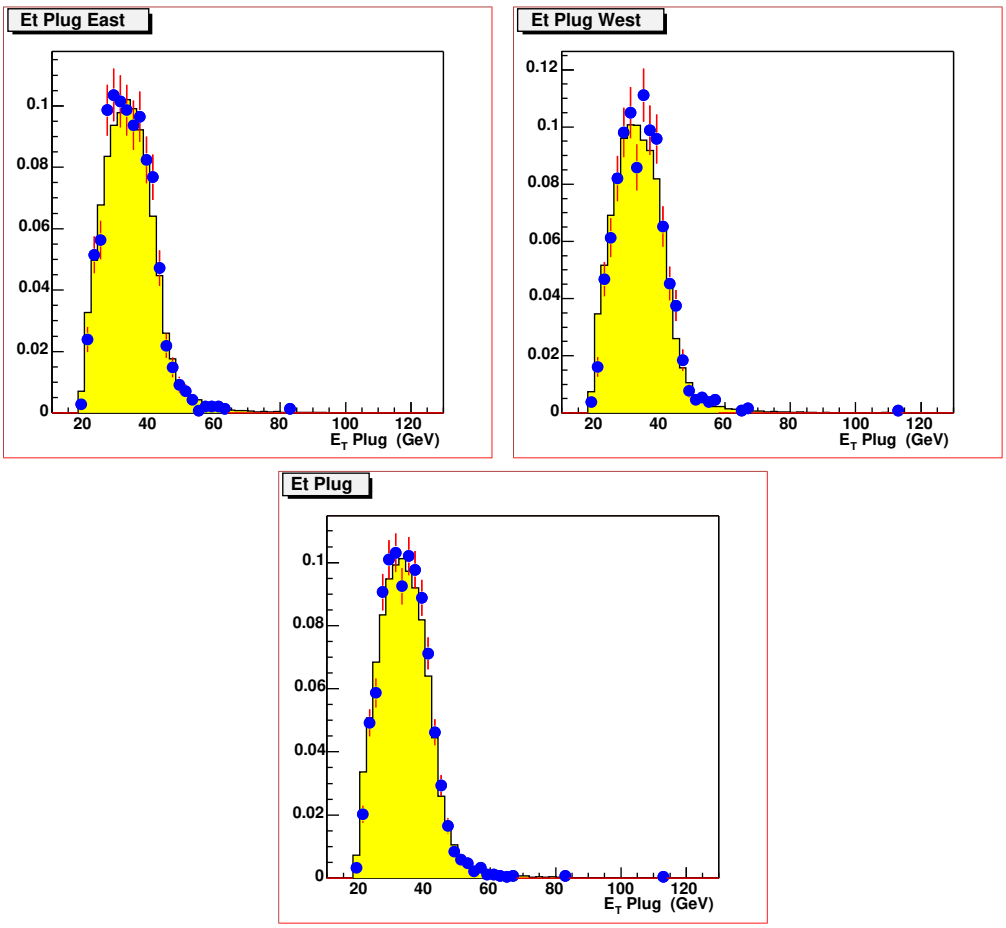

Figure 21: *E_T distribution of the plug leg in $Z \to ee$ CP candidates. Data (dots) and MC superimposed.*

points in χ^2 fit between data and MC invariant mass distribution of $Z \to ee$ [6] . The largest difference between the $\pm 3\sigma$ acceptances and the mean value was taken as systematic uncertainty, its value is 0.0011 (ΔA/A (%) = 0.353) for scale and 0.0005 (ΔA/A (%) = 0.16) for resolution.

Four parameters (PARP(62),(64),(91) and (93)) of Pythia are used to tune $d\sigma/dp_T$ distribution of ee pairs in mass window $66 < M_{ee} < 116\ GeV$. For each

of the four parameters, distributions are produced by varying values of the parameter and compared with CDF's RunI data by χ^2. The uncertainty on P_T modeling is obtained by $\pm 3\sigma$ values in χ^2 fit and taking the largest variation in acceptance for each of them [9]. Total uncertainty for P_T modeling is obtained by adding in quadrature all variations, see table 3.

Parameter	Δ Acceptance/A (%)
PARP(62)	0.01
PARP(64)	0.04
PARP(91)	0.04
PARP(93)	0.00
Total	0.057

Table 3: The uncertainty in $W \to e\nu$ acceptance for tuned Pythia p_T W parameters.The largest variation from $\pm 3\sigma$ is considered.

Effect of extra material on acceptance was calculated by using a special MC sample with $\pm$ 1.5% X_0 of material (copper) between the beam line and the COT inner cylinder (corresponding to $\pm 1\sigma$) and $\pm$ 1/6 X_0 of material (iron) in front of the plug calorimeters. The largest difference in acceptance is taken as the corresponding systematics. The effect of extra material in central region is negligible. The results of extra material studies are summarized in table 4.

MC dataset	Description	Δ Acceptance	Δ A/A (%)
wewk3e	+ 1.5% of X_0 Cu in central	0.00003	-
wewk4e	- 1.5% of X_0 Cu in central	0.00002	-
wewkae	+ 1/6 of X_0 Fe in plug	0.0028	0.90
wewk6e	- 1/6 of X_0 Fe in plug	0.0026	0.84
Total			0.90

Table 4: Change in acceptance for extra material.

Energy recoiling against the W ($\vec{U} = -M\vec{E}T - \vec{E_T^e}$) was studied in data and MC (see Figs. from 22 to 27). In order to obtain a better agreement with the data, the MC $\vec{U}$ was scaled (by 1.09) and shifted in parallel (by -0.465) and perpendicular (by 0.006) direction with respect to the lepton direction. The effect of a possible mis–modeling of $\vec{U}$ on the acceptance calculation was estimated by taking the $\pm 3\sigma$ variation, where σ was computed by studying the χ^2 distribution of the $\vec{U}$ variables (see table 5).

We took the quadratic sum of the largest changes in acceptance as systematic uncertainty.

Parameter	Scale $\lvert\vec{U}\rvert$	Scale $U_{\parallel}$	Scale $U_{\perp}$	Shift $U_{\parallel}$	Shift $U_{\perp}$
ndf	200	200	200	200	200
Fit value	1.069	1.097	1.104	-0.465	0.006
$\Delta value_{\pm 3\sigma}$	0.027	0.034	0.037	0.153	0.151
$\Delta A/A_{+3\sigma}(\%)$	0.18	-	-	0.29	0.004
$\Delta A/A_{-3\sigma}(\%)$	0.17	-	-	0.3	0.005
Total	0.35				

Table 5: Results of χ^2 fits in uncertainty study of recoil energy.

The effect of the choice of Parton Distribution Functions (PDFs) in the MC was studied by using CTEQ6 PDF described by 20 parameters. For each parameter samples corresponding to $\pm 1\sigma$ change of parameter were generated, referred to as the error PDF sets. Using 40 error sets and one central PDF, 41 samples of $W \to e\nu$ samples were produced, see [9] and citation therein. For each sample acceptances are calculated using central (A_0) and i-th error PDF (A_i) sets where even (odd) i corresponds to a $+1\sigma$ (-1σ) variation. The asymmetric uncertainty in the Parton Distribution Function (Err^+_{PDF}, Err^-_{PDF}) is estimated from the deviations from the default acceptance value:

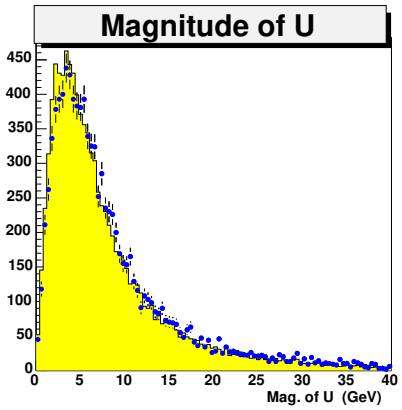

Figure 22: *Data (points) and MC (histogram) comparison for $|\vec{U}|$ not tuned.*

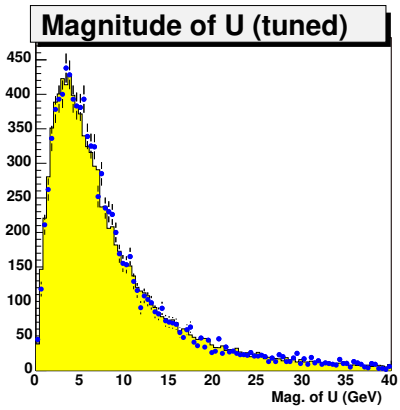

Figure 23: *Data (points) and MC (histogram) comparison for $|\vec{U}|$ tuned.*

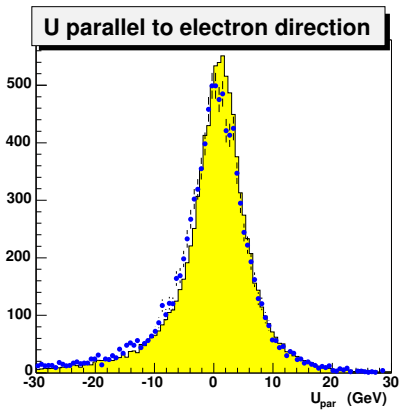

Figure 24: *Data (points) and MC (histogram) comparison for $U_{||}$ not tuned.*

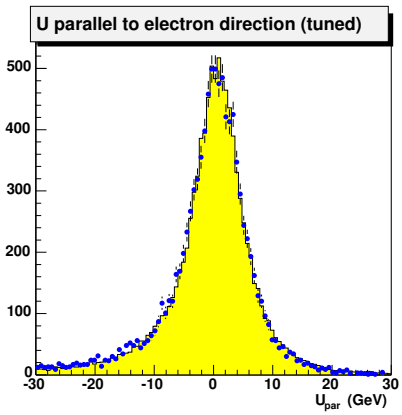

Figure 25: *Data (points) and MC (histogram) comparison for $U_{||}$ tuned.*

$$t_+ = A_{2i} - A_0 \quad ; \quad t_- = A_{2i+1} - A_0$$

$$Err^+_{PDF} = \sqrt{\sum_{i=1}^{20} P_i} \quad ; \quad Err^-_{PDF} = \sqrt{\sum_{i=1}^{20} M_i}$$

(P_i, M_i)	$t_+ < 0$	$t_+ > 0$
$t_- < 0$	$\left(\frac{1}{2}(t_+^2 + t_-^2), 0\right)$	(t_+^2, t_-^2)
$t_- > 0$	(t_-^2, t_+^2)	$\left(0, \frac{1}{2}(t_+^2 + t_-^2)\right)$

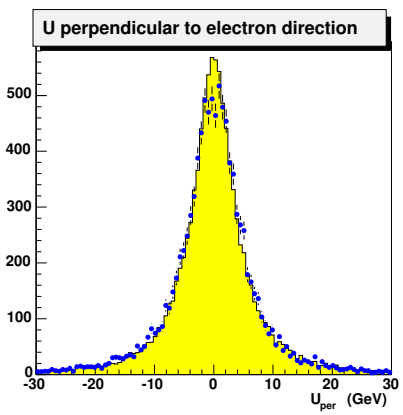

Figure 26: *Data (points) and MC (histogram) comparison for $U_\perp$ not tuned.*

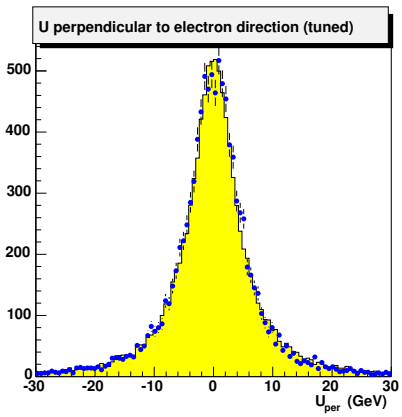

Figure 27: *Data (points) and MC (histogram) comparison for $U_\perp$ tuned.*

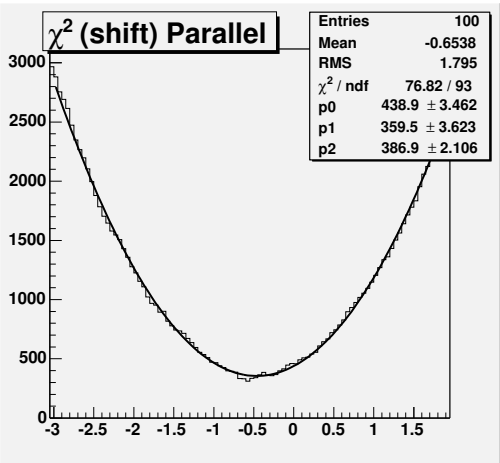

Figure 28: χ^2 *for* $U_\parallel$ *(shift).*

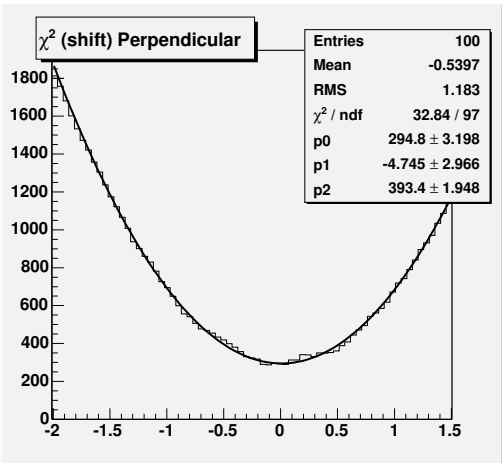

Figure 29: χ^2 *for* $U_\perp$ *(shift).*

The overall uncertainty is summarized in table 6.

5 Primary Vertex Finding Efficiency

The efficiency for reconstructing a primary vertex was estimated by using a sample of events $Z \to ee$ CP where the primary vertex was found within 60cm from the nominal z primary vertex (z=0). After selection of the sample, events were stripped

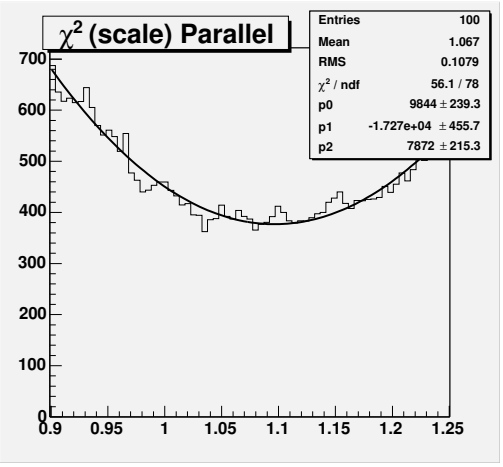

Figure 30: χ^2 *for* $U_{||}$ *(scale).*

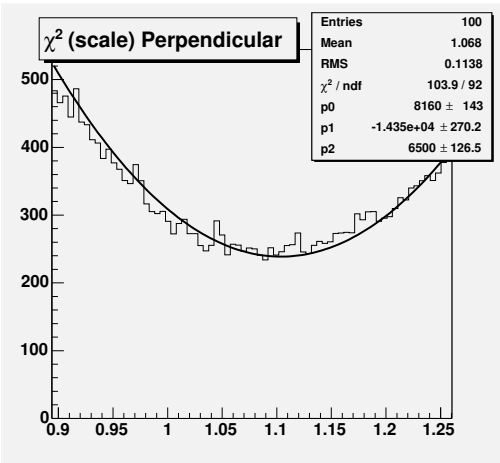

Figure 31: χ^2 *for* $U_{\perp}$ *(scale).*

Source	Syst. uncertainty (%)
plug E_T^e scale	0.35
E_T^e resolution	0.16
P_T^W	0.06
$\vec{U}$	0.35
Material	0.90
PDF's	+1.7 -1.4
Total	+2.0 -1.7

Table 6: Systematic uncertainty on the acceptance.

of the central leg and reprocessed through production. Figure 35 shows the difference between the original z of the primary vertex and the z obtained after reprocessing. Requiring that the primary vertex after stripping off the central track associated to the central *tight* electron was found within 60cm of the nominal point of interaction we measure an efficiency of: $\epsilon_{|PVz|<60\text{cm}} = 92.0 \pm 0.5(\text{stat})\%$.

The shift in the primary z vertex position alter some quantities used in the selection of candidates (E_T, track momentum, ...) that are recalculated with respect to the primary vertex obtained without the central track. The variation in the

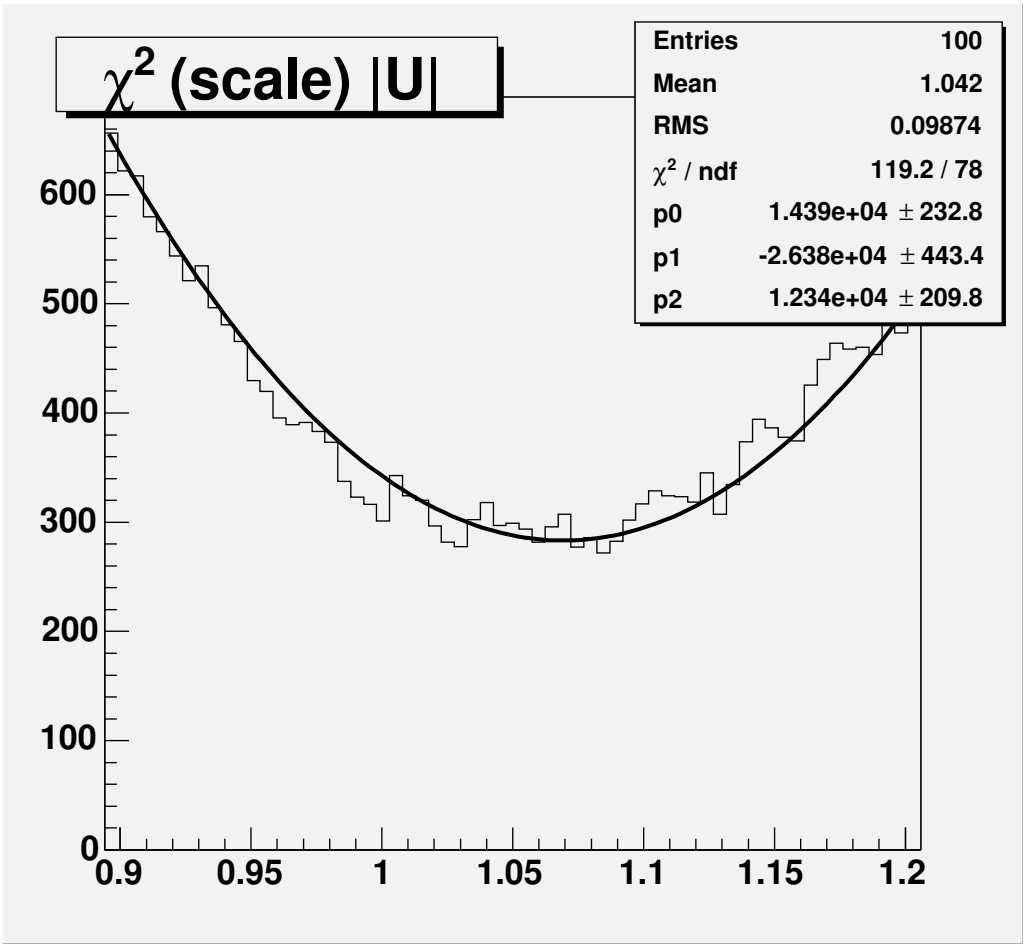

Figure 32: χ^2 *for* $|\vec{U}|$.

acceptance (0.35 %) is taken as systematic uncertainty in the acceptance.

6 Electron ID Efficiencies

Thanks to the use of tracking we were able to keep the requirements needed to identify an electron at a minimum, therefore only Had/Em and IsoRel cuts were applied. In both cases, to measure the efficiencies in data, we used the unbiased

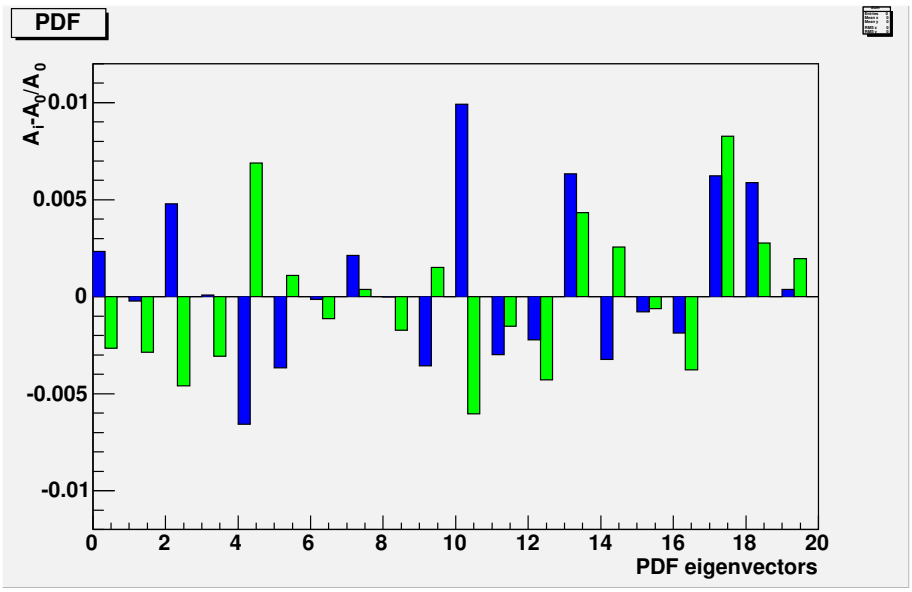

Figure 33: *The Relative variations of acceptance for different error PDF sets.*

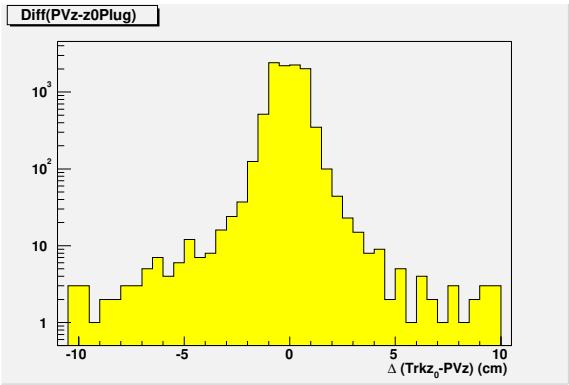

Figure 34: *Difference between z_0 of matched track to the plug with Primary Vertex found by* ZVertexColl *on $W\rightarrow e\nu$ candidate events.*

plug leg of our CP Z sample. Efficiency to pass cut i is defined as the number of electron candidates passing cut i divided by the number of candidates passing all other (but the i^{th}) cuts.

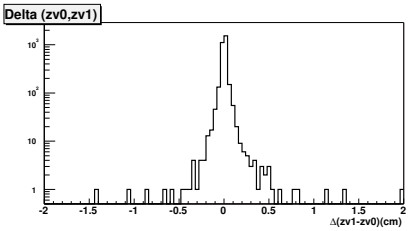

Figure 35: *Difference between primary vertex Z in $Z \rightarrow ee$ CP events before and after removing the central leg.* $|\Delta(zv_1, zv_0)| < 2cm$

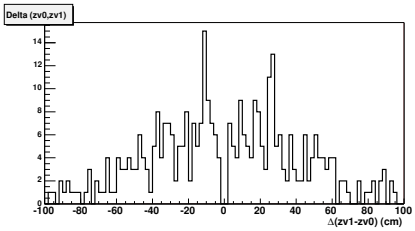

Figure 36: *Difference between primary vertex Z in $Z \rightarrow ee$ CP events before and after removing the central leg.*$|\Delta(zv_1, zv_0)| > 2cm$

Dijet events are the dominant source of background and were subtracted from our sample. We followed the same method used in [6][7]. From *jet20* sample `gjet0a` Z and W candidates were removed by requiring no more than one loose electron and $\not\!\!E_t < 15$ GeV. The fake rate is defined as the fraction of jets in the sample passing electron-selection criteria. On Fig.38 (Fig.37) fake rates are shown for jets before (after) passing ID selection criteria. The fake rates for central tight electron are identical with those found by [6]. After obtaining the fake rates we go through the jet sample and select events with central jet (with $E_T > 25GeV$) and plug jet (with $E_T > 20GeV$). Invariant mass distributions from selected central-plug events were weighted by product of appropriate (central and plug) fake rates. To obtain the expected number of background events, the integrals of the dijet invariant mass in the $80 < M_{jj} < 100$ mass window for denominator and numerator were multiplied by a factor 384 [6] that takes into account the prescale for JET20 trigger path. A 30 % systematic uncertainty is estimated on the fake rates. The final ID efficiency was calculated with:

$$\epsilon_{ID,Bkg\,removed} = \frac{\text{Numerator} - \text{Bkg}_{\text{Num}}}{\text{Denominator} - \text{Bkg}_{\text{Denum}}};$$

and is: $96.1 \pm 0.4(\text{stat}) \pm 2.2(\text{syst})$. Results are shown in table 8.

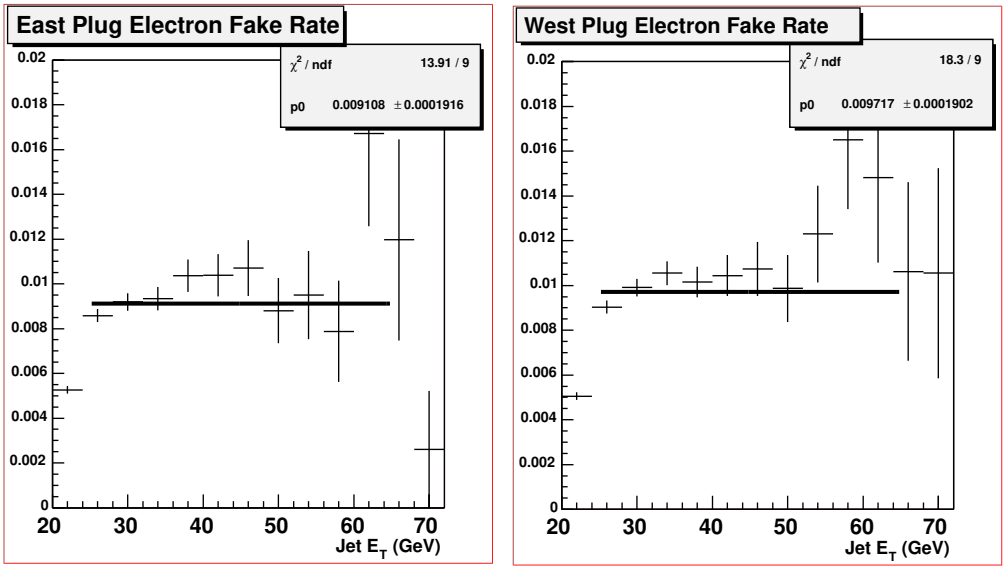

Figure 37: Fake Rates *vs* E_T of jet for East (left) and West (right) plug electron after ID cuts (Tab.7).

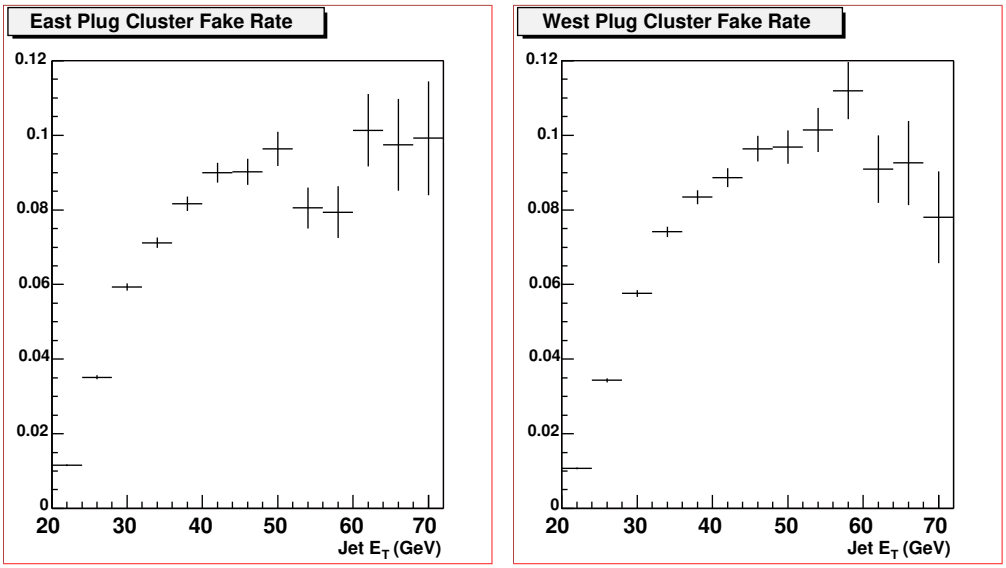

Figure 38: Fake Rates *vs* E_T of jet for East (left) and West (right) Plug electron before ID cuts (Tab.7).

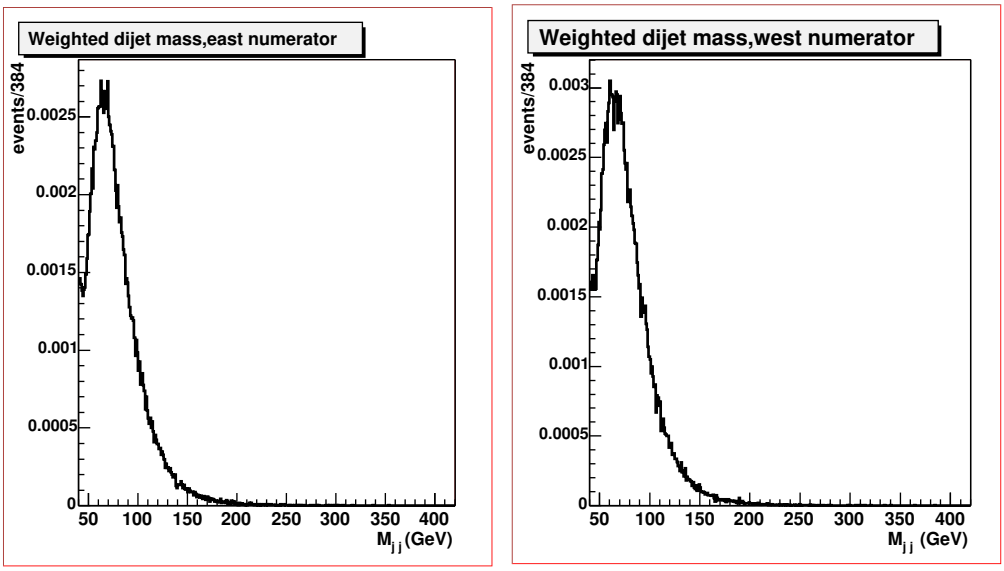

Figure 39: Invariant dijet mass obtained weighting jets with fake rate (Fig.37).

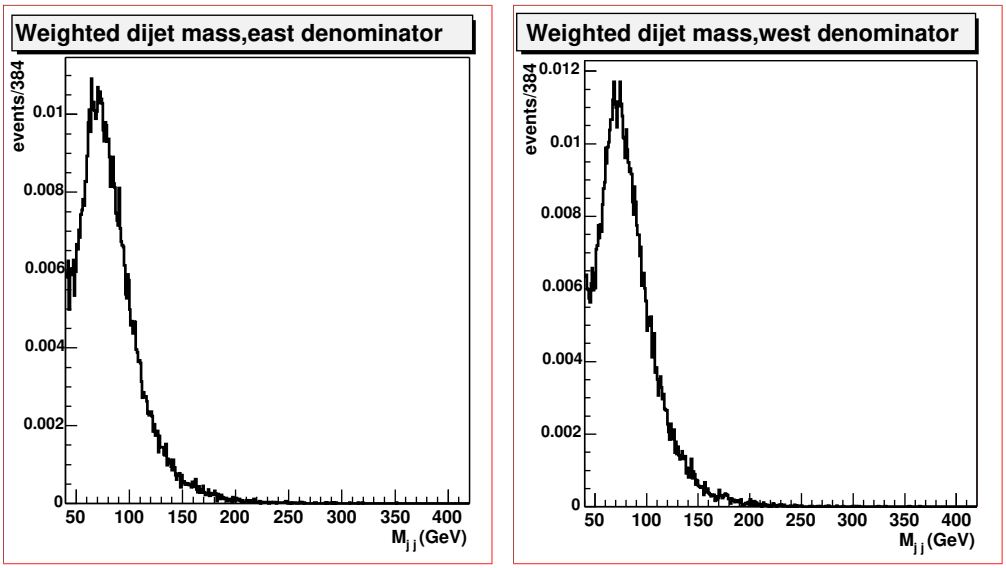

Figure 40: Invariant dijet mass obtained weighting jets with fake rate (Fig.38).

cut	ϵ (75-105 GeV/c^2)	ϵ (80-100 GeV/c^2)
Had/Em < 0.05	0.957 ± 0.004	0.967 ± 0.004
IsoRel< 0.1	0.934 ± 0.004	0.946 ± 0.004
ϵ_{ID} combined	0.914 ± 0.005	0.929 ± 0.005

Table 7: Efficiencies of Had/Em and IsoRel without QCD background subtraction.

	Cand Events	Bkg QCD (syst)
East Numerator	1420	11 ± 5
East Denominator	1510	58 ± 25
West Numerator	1305	13 ± 6
West Denominator	1422	63 ± 26
ϵ_{ID}	96.1 ± 0.4(stat) ± 2.2(syst)	

Table 8: Efficiencies of ID selection after background subtraction with $80 < M_{ee} < 100$ invariant mass window.

7 Trigger Efficiencies

The efficiency of the MET_PEM trigger path was extensively studied and is the subject of a separate note [11] where we also report value of the turn on curves and our studies about time dependence of the efficiencies. In the following we summarize our studies and report only the results relevant to the data taking period used in this measurement.

The efficiency of the various levels was studied using backup trigger paths, see table 9, where we also show the trigger path (MET_PEM) of our data set. We applied to all data the selection criteria used in this analysis, and studied the various efficiencies as a function of the appropriate variable.

Looking at the table is clear that one can measure (and study as function of MET) a combined efficiency of $L1_MET15\&L3_MET15$ and then check, in-

Trigger Path	level	Triggers
MET_PEM	L1	L1_EM8_MET15
	L2	L2_PEM20_L1_EM8_MET15
	L3	L3_PEM20_MET15
PLUG_ELECTRON_20	L1	L1_EM8
	L2	L2_PEM20_PS10
	L3	L3_PEM20
MET_PEM_L1_EM8_MET15	L1	L1_MET15
	L2	L3_PSX_L1_EM8_MET15
	L3	L3_PEM20_MET15
JET_20	L1	L1_JET5
	L2	L2_PSX_L1_JET5
	L3	L3_JET_20

Table 9: List of Trigger Paths considered.

dipendently, that indeed its value is the product of the two separate efficiency for $L1_MET15$ and $L3_MET15$). Therefore we measure the combined $L1_MET15$ and $L3_MET15$ trigger efficiency by calculating the following ratio:

$$\epsilon(L1_MET15 \& L3_MET15) = \frac{P_20 \& MET_PEM}{P_20}$$

Then one can measure the $L1_MET15$ only, under the assumption that $L1_EM8$ is 100% efficienct, by looking at the ratio of events:

$$\epsilon(L1_MET15) = \frac{P_20 \& L1_EM8_MET15}{P_20}$$

Finally the $L3_MET15$ trigger efficiency can be measured by looking at the ratio:

$$\epsilon(L3_MET15) = \frac{P_20 \& L2_PEM20_L1_EM8_MET15 \& MET_PEM}{P_20 \& L2_PEM20_L1_EM8_MET15}$$

where we have called P_20 the $PLUG_ELECTRON20$ trigger.

In figure 41 we show the L1 trigger efficiency as a function of MET. An overall $\epsilon_{L1} = 0.995 \pm 0.003$ is found in data.

In a similar fashion, L2 is studied by looking at our candidate events passing an auto accept (prescaled) L2 trigger, $L2_PS_X_L1_EM8_MET15$ where X = 10 or

	$\epsilon(L1_MET15\&L3_MET15)$	$L1_MET15$	$L3_MET15$	$L1_MET15 \times L3_MET15$
Num	970	971	970	N/A
Denum	975	975	971	N/A
Eff	0.995 ± 0.003	0.996 ± 0.2	0.999 ± 0.001	0.995 ± 0.3

Table 10: L1_MET15_L3_MET15 Trigger efficiencies

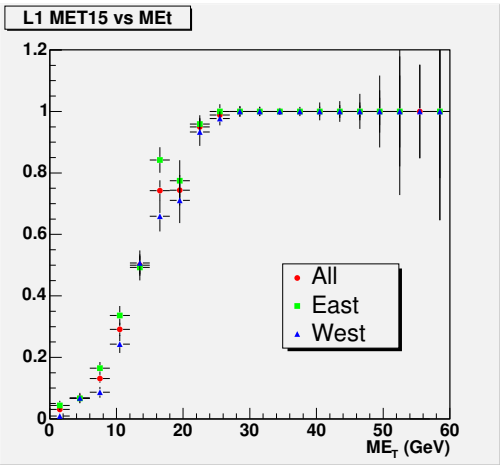

Figure 41: $L1_MET15$ *efficiency vs MET.*

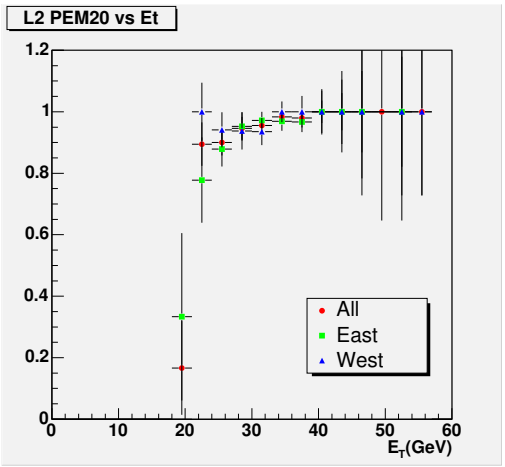

Figure 42: *L2 efficiency vs* E_T.

20 depending upon the trigger table. Figure 42 shows its behaviour as a function of E_T. The trigger turn on due to the E_T threshold is clearly visible. The L2 trigger efficiency is $\epsilon_{L2} = 0.963 \pm 0.011$.

Finally L3 trigger efficiency is measured by looking at the plug leg of the $Z \rightarrow ee$ CP candidates. A total of 75/75 events (32/32 and 43/43 for east and west respectively) and $\epsilon_{L3} = 1^{+0.0}_{-0.01}$.

Table 11 summarizes our results, we also provide the value of the same trigger efficiencies if we loosen the E/p cut.

We checked the trigger efficiencies using a different data sample (dijet in the plug). We selected 19 events based on our analysis, 16 of which passed the MET_PEM trigger path. The result is a global efficiency of ϵ_{MET_PEM} of 0.842 ± 0.094. East side has an efficiency of $9/10 = 0.90 \pm 0.13$ and the West side $7/9 = 0.78 \pm 0.16$.

Trigger level	ϵ w/o E/p	ϵ $0.5 < E/p < 4$	ϵ $0.5 < E/p < 2$
Level 1	0.975 ± 0.003	0.976 ± 0.003	0.995 ± 0.003
Level 2	$0.964. \pm 0.0082$	0.964 ± 0.009	0.963 ± 0.011
Level 3	$1.0^{+0.00}_{-0.01}$	$1.0^{+0.00}_{-0.01}$	$1.0^{+0.00}_{-0.02}$
Overall	0.940 ± 0.009	0.940 ± 0.009	0.958 ± 0.012

Table 11: Trigger efficiencies.

Given the large statistical uncertainties we can just conclude that these results are consistent with our measurement obtained with backup triggers.

8 Tracking Information and Tracking Efficiencies

This analysis is largely based on the use of the Standalone Silicon Tracking algorithm which was optimized on MC and never validated using data. Therefore the existence of possible discrepancies between data and MC is not surprising. Also, the ISL $R-Z$ alignment is still in progress and stereo layers play a very important role in the pattern recognition. For this analysis we choose to rely on data as much as possible.

A first check is the comparison of reconstructed electron tracks ("plug leg") in $Z \to ee$ CP events in data and MC as discussed in previous section.

Fig. 18 through 21 show several distributions (data and MC normalized to 1).

We now define tracking efficiency as the probability to associate a track to an EM cluster passing all selection criteria and to extrapolate to a PES cluster with a ΔX,ΔY (PES-extrapolated track) to better than 3 cm. By definition a photon converting at radius larger than a few cm will generate some inefficiency. On the other side, as we require a mild isolation, charged tracks overlapping with photons from π^0 will contribute positively to the overall efficiency.

Using MC $W \to e\nu$ events the reconstruction efficiency is 0.4138 ± 0.0014. The fraction of events with an *EM* cluster matched to a track in data is 0.201 ± 0.007.

We notice that, although in data there is still a large background contribution as discussed in previous section, the two figures largely disagree.

We believe that this is partly due to ladders which were not integrated during data taking and partly due to a still preliminary capability of the MC to emulate fine details of the response of the SVX and ISL. Details which play a pivotal role in the reconstruction efficiency. While the best way is eventually to be able to reproduce all features of data in MC, at this moment we prefer to use data to obtain an estimate of tracking efficiency in W events. Therefore we define the tracking efficiency in W events as:

$$\epsilon_{tracking} = \epsilon_{W_{MC}} \times ScaleFactor$$

where:

$$ScaleFactor = \epsilon_{Z_{data}}/\epsilon_{Z_{MC}}$$

Using MC $Z \to e^+e^-$ events and 3077 candidate events in CP Z data, in the ee invariant mass window 80–100 GeV/c^2, we obtain a SF of 0.772 ± 0.02.

Fig. 43, 44, 45 show comparisons of tracking efficiency as a function of φ, η, and electron E_T for data and MC in $Z \to ee$ events.

It is clear that there is an η dependence of the scale factor. However the difference between W and Z events is small, as can be seen in figure 46 where we compare the η and E_T distribution for the plug leg of $Z \to ee$ data events with the same quantities for our W candidates. The η distributions for the two sets are essentially the same, differences well within statistics. A difference of less than 5% can be seen in the E_T as expected due to the difference of the two spectra.

Using a scale factor self-defined by data, we automatically correct -on a run by run basis- for difference in silicon acceptance. However we have a way, in principle, to improve data and MC comparison by requiring -for a given candidate EM cluster- all silicon layers to be readout for that specific event. This is done by a module written for this purpose, which first defines a *road* using the EM cluster energy and the z of the primary vertex. Then the code checks the (individual) status of each

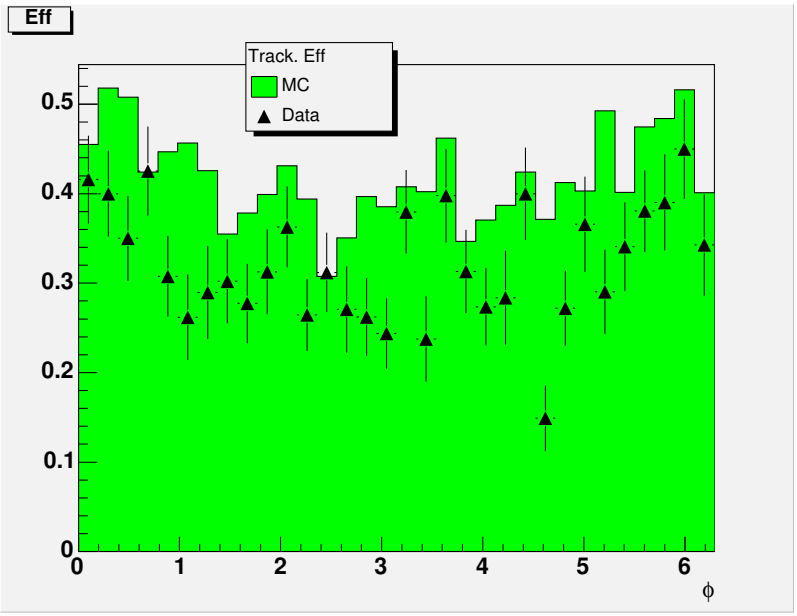

Figure 43: *Tracking efficiency of plug leg in Z events as a function of φ. Data and MC (green histogram) comparison.*

crossed silicon layers. By comparing tracks in which all crossed layers were active in data with MC events, we hope to improve understanding of the disagreement.

Plots showing the behaviour of the Scale Factor as a fucntion of E_T, η and φ are shown in figure 47, 48, 49.

As the E_T dependence seems to be the only one where Z and W events differ, we estimated the effect due to the use of a flat scale factor rather than using a scale factor varying with energy. We divided the W candidates in different electron E_T bins and corrected each one with the appropriate (for that energy bin) scale factor. The difference between this result and what obtained by using a flat scale factor is $\Delta_{SF} = 0.019$. We take the absolute value $|\Delta_{SF}|$ as systematic uncertainty on the scale factor.

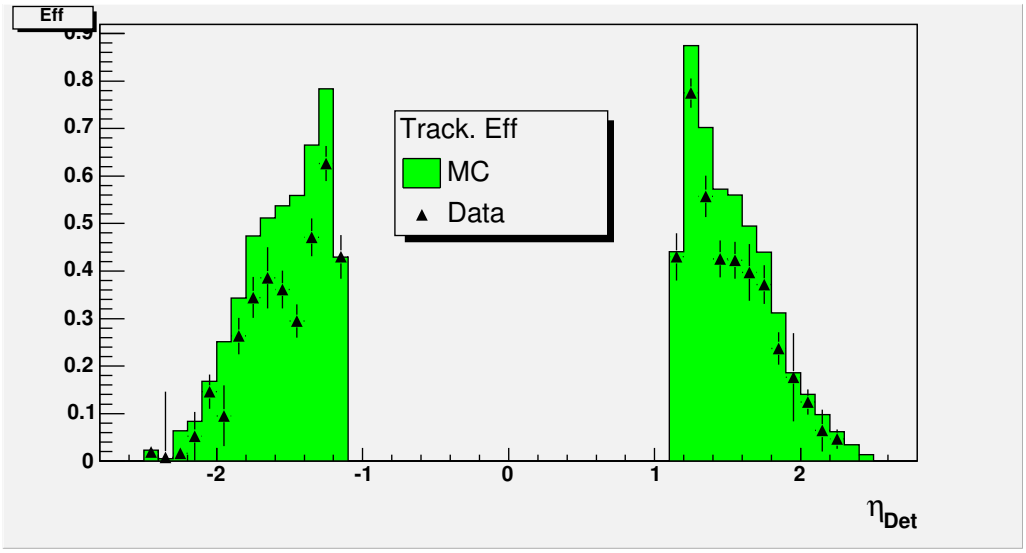

Figure 44: *Tracking efficiency of plug leg in Z events as a function of η. Data and MC (green histogram) comparison.*

9 E/p

Using the plug leg of $Z \to ee$ sample (mass window 80-100 GeV/c^2) we measure the efficiency of E/p requirement to be 0.639 ± 0.015 (figure 50).

Numerator and denumerator are corrected by the QCD background contamination evaluated with the method described in Sec.6. The source of systematic uncertainty is related to the background uncertainties affecting both numerator and denominator. We estimate the uncertainty to be: $\pm$ 0.001. [1]

10 Background

QCD background is computed in the usual way. Studying the MET vs IsoRel plot (figure 51), one defines four regions:

[1] However, removing the $E/P < 0.5$ selection an difference of 0.008 is observed. We quote this latter as the systematic uncertainty of the E/P selection

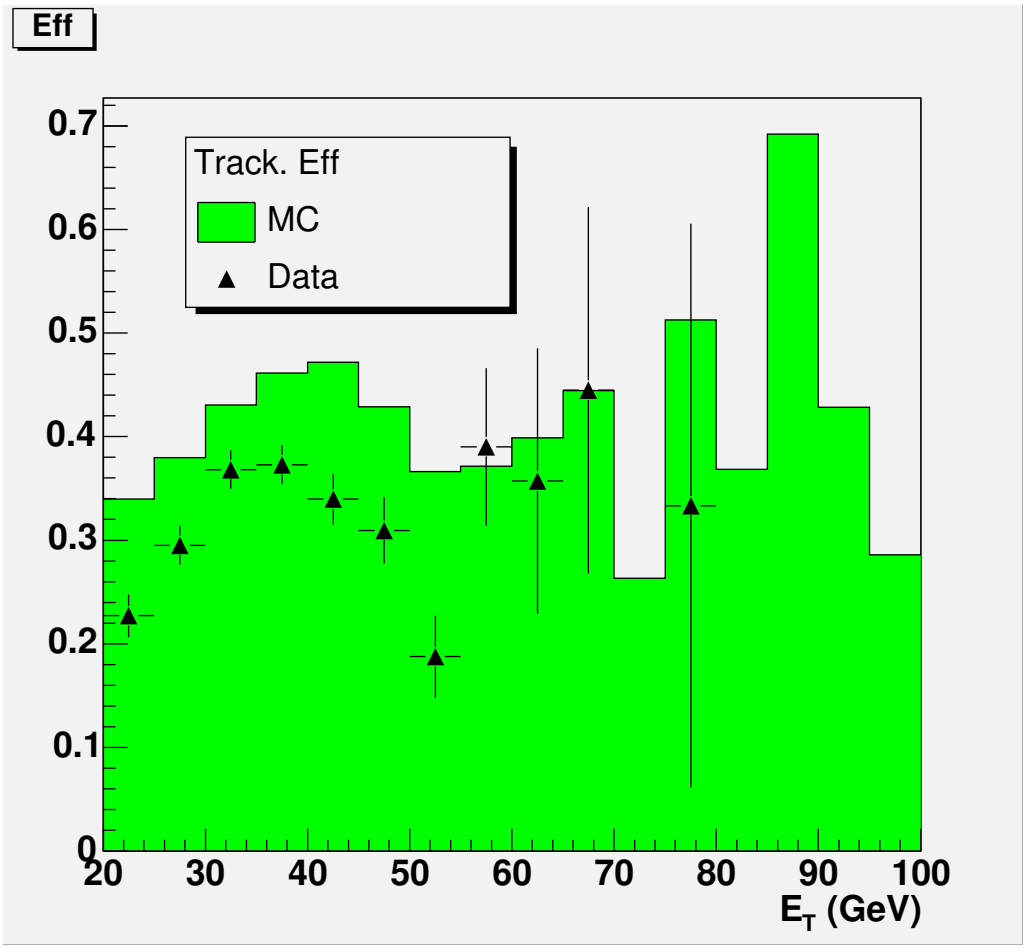

Figure 45: *Tracking efficiency of plug leg in Z events as a function of E_T. Data and MC (green histogram) comparison.*

- region A: MET <10 GeV, IsoRel < 0.1;
- region B: MET <10 GeV, IsoRel > 0.2;
- region C: MET >20 GeV, IsoRel > 0.2;
- region D: MET >20 GeV, IsoRel < 0.1.

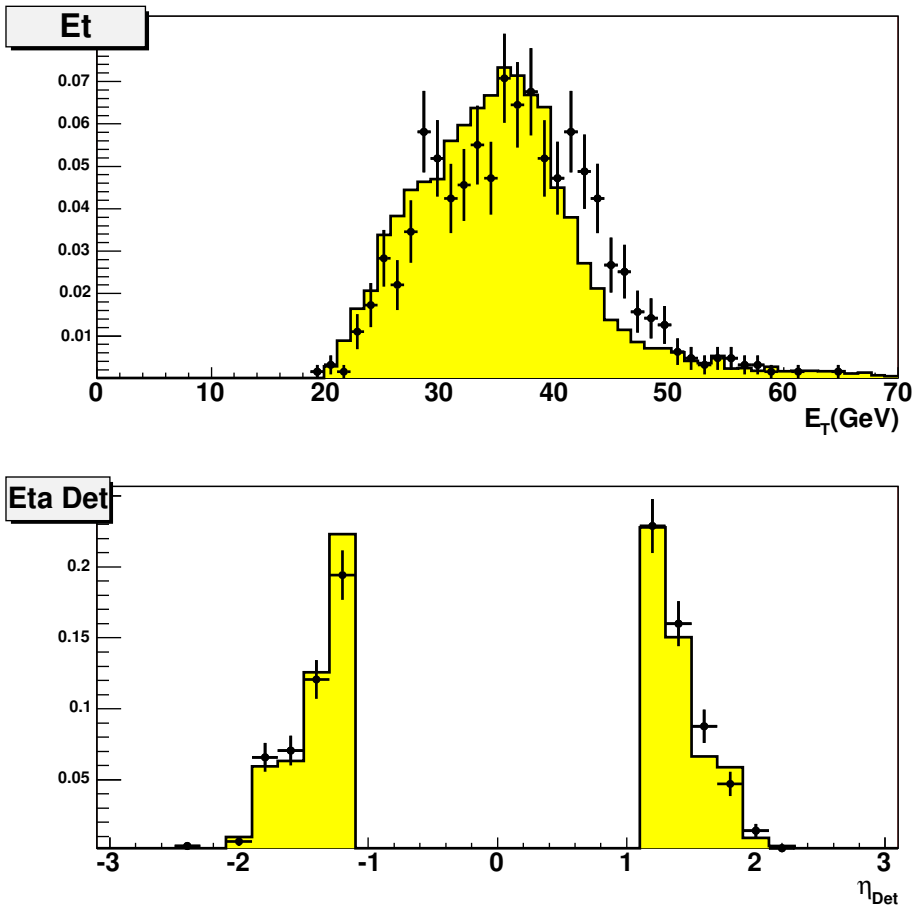

Figure 46: *Comparison of η and E_T distribution for electron candidates in W (histograms) and Z (dots) events.*

Signal region is D. The number of backgound events in this region is given by the following equation:

$$N_{bckg} = N_A \times \frac{N_C}{N_B}$$

Shape of background is provided by events in region C. In our sample, the total number of expected QCD background events is 643 ± 62(stat.). This number, which we can call *raw QCD* background has to be corrected for signal contribution as well

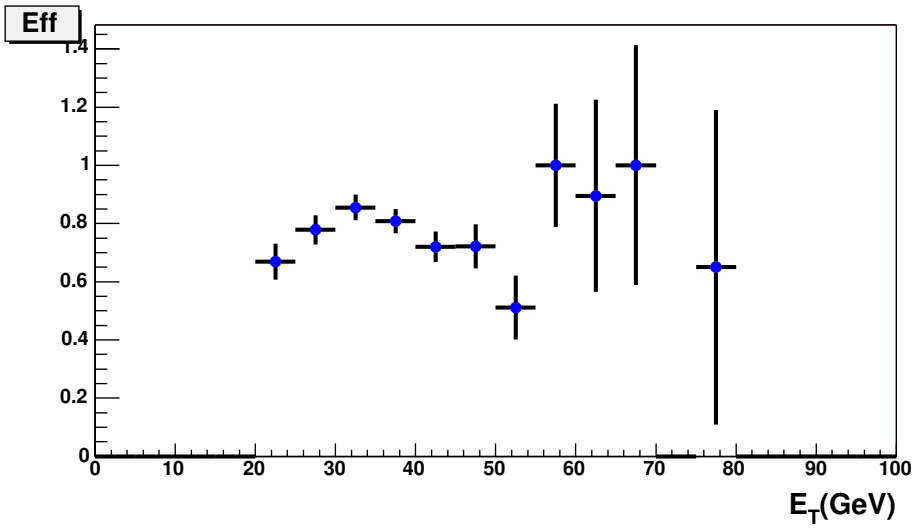

Figure 47: *Scale Factor as a function of electron* E_T.

as for $Z \to ee$ and $W \to \tau\nu$ which are computed separately. When we apply the corrections relative to those contributions, the final QCD background is 495 events. To be conservative we assign to this number the uncertainty obtained for the *raw QCD* background.

In order to estimate the systematic uncertainty of the *raw QCD* background estimate obtained using this technique, we varied the position of the IsoRel and MET cuts which define the four regions.

Figure 52 shows the dependence of the background estimate on the values of the IsoRel and MET cuts. The background estimate seems to depend on the IsoRel value more than on the MET cut, although the last three points of figure 52, upper plot, are clearly statistically limited. We conservatively assume that the systematic error of the QCD background obtained using the IsoRel vs MET method is about 50%.

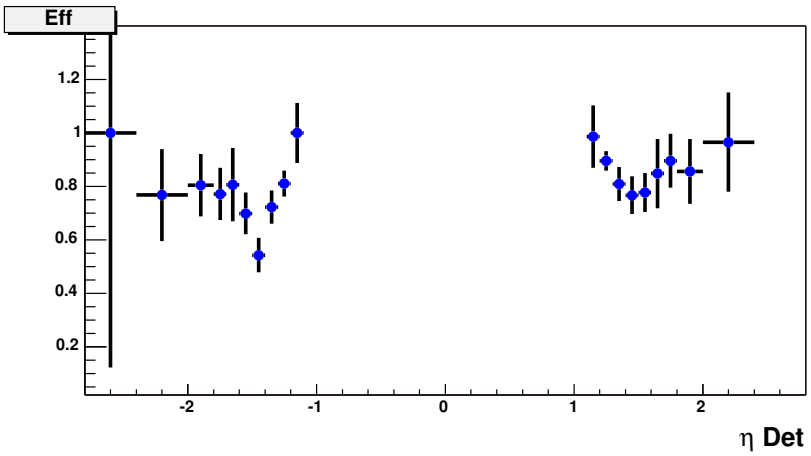

Figure 48: *Scale Factor as a function of electron η.*

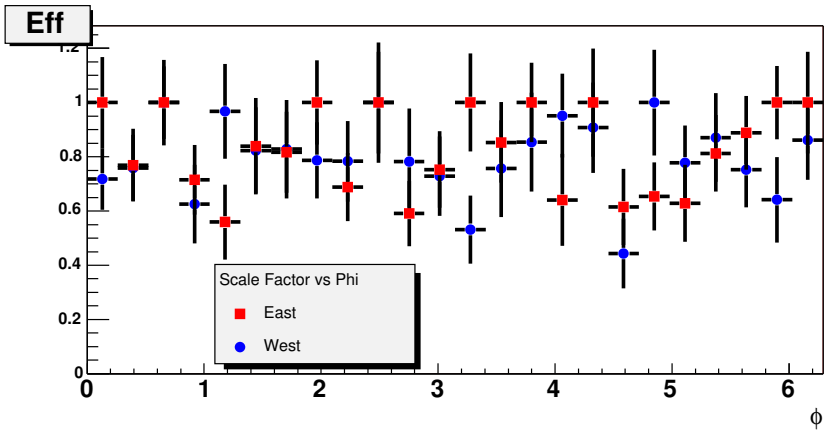

Figure 49: *Scale Factor as a function of electron φ. East and West divided.*

Other background contributions come from the $W \to \tau\nu$ and $Z \to ee$ events. Transverse mass shape for the two samples is obtained by MC.

Normalization is obtained in the following way. For $W \to \tau\nu$ case we looked at Monte Carlo events passing our selection criteria.$(0.32 \pm 0.02\%)$ of Monte Carlo events survive our analysis chain. Therefore, as the cross sections for the two leptonic

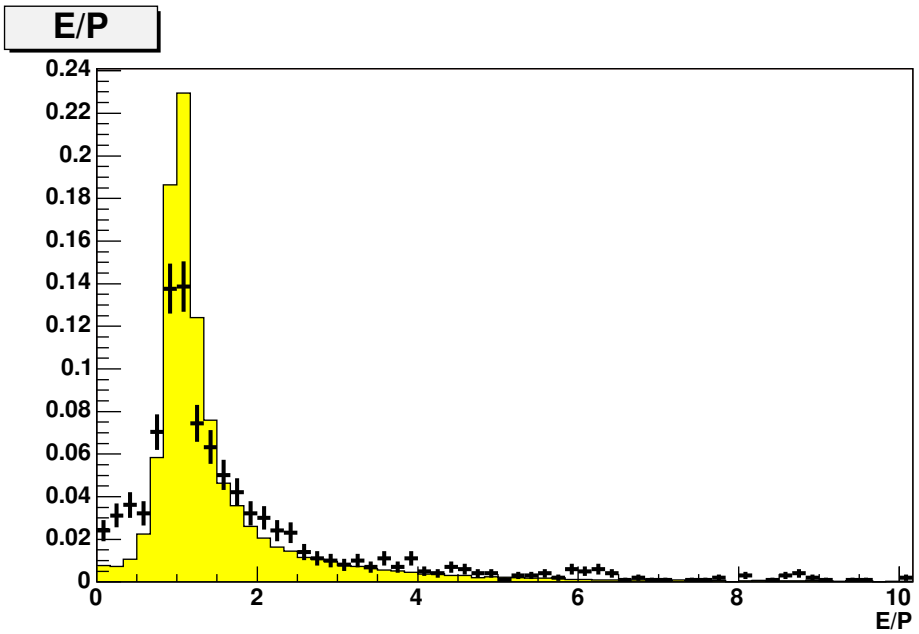

Figure 50: *E/p for the plug leg of $Z \to ee$ CP. Data and MC comparison.*

final states are equal:

$$N_{W\tau} = (N_C - N_O - N_{W\tau})/R(W_e/W_\tau)$$

where N_C is the number of W candidates in our sample, N_O is the estimated QCD background plus the contribution from $Z \to ee$ and $R(W_e/W_\tau)$ is the ratio of acceptances times cross sections (assumed to be identical). In this ratio the scale factor (data/Monte Carlo) for the tracking efficiency in the two samples is assumed to be identical.

In a similar way the number of Z in our final sample is obtained by applying all our analysis cuts to a MC Z sample. The efficiency for Z events is $(0.92 \pm 0.01)\%$. The number of Z in our final sample is estimated by:

$$N_Z = (N_C - N_O)/(R(W_e/Z_e) + 1)$$

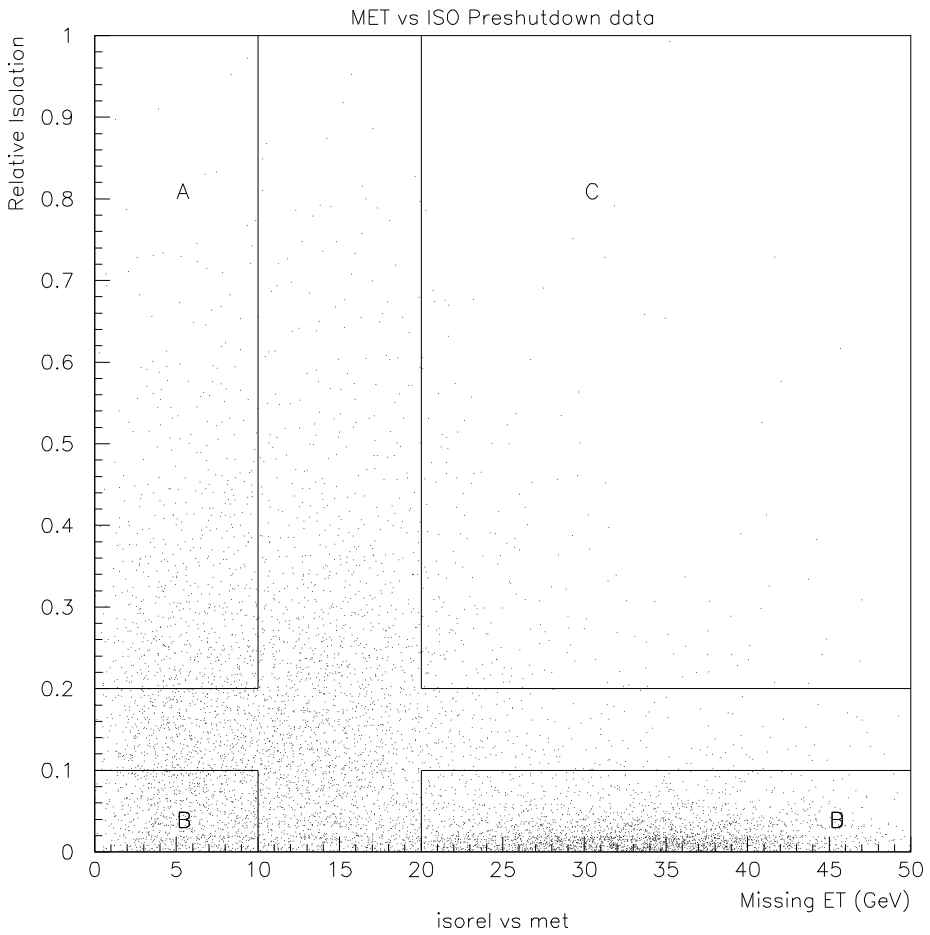

Figure 51: *Relative Isolation vs MET.*

where N_C is the number of candidates, N_O is the sum of QCD and $W \to \tau\nu$ contribution, R is the ratio of acceptances times cross sections of $W \to e\nu$ and $Z \to ee$ events. As ratio of cross sections we take 10.66 ± 0.05 (NNLO value) [10]. In this case, the scale factor is identical by construction. By solving the equations we find the contribution to background coming from the two processes (325 events from $W \to \tau\nu$ and 87 from $Z \to ee$). Figures 53, 54, 55 show data overlayed to expected

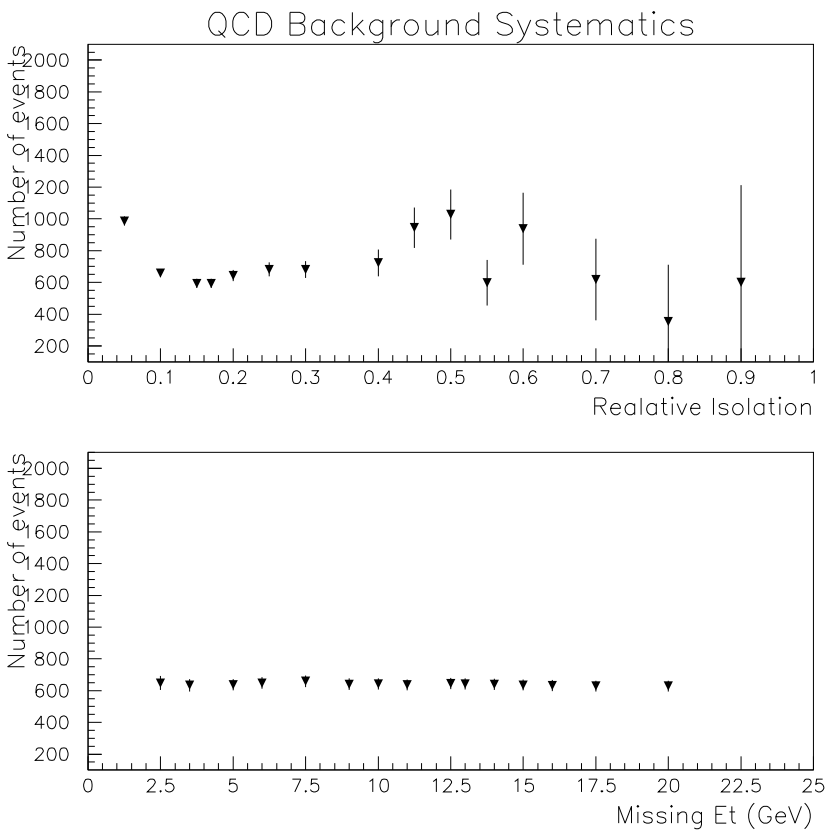

Figure 52: *QCD background dependence on the Isolation fraction and MET cut values which define the control regions.*

yield of events after taking into account background contributions. We recall here that the energy was corrected using the values found by the $Z \to ee$ CP analysis [4].

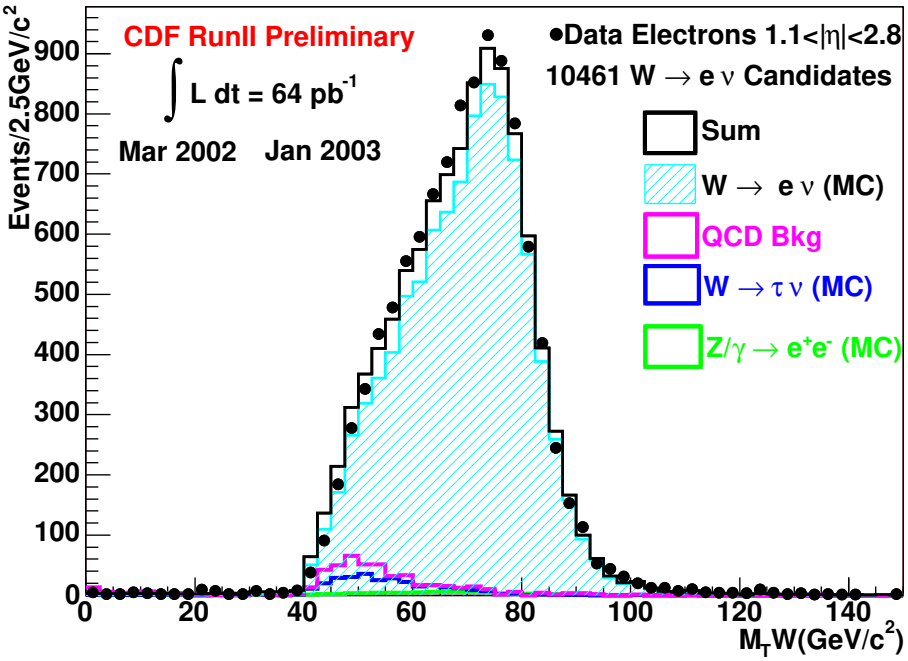

Figure 53: *Transverse mass of W candidates compared to expected signal.*

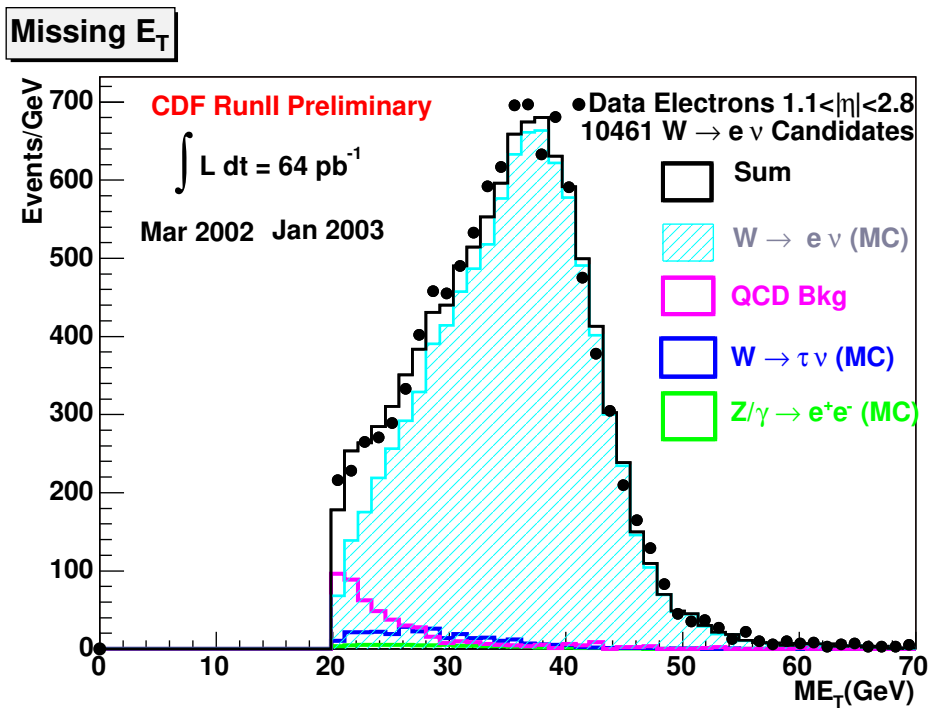

Figure 54: *MET in W candidate events compared to expected signal.*

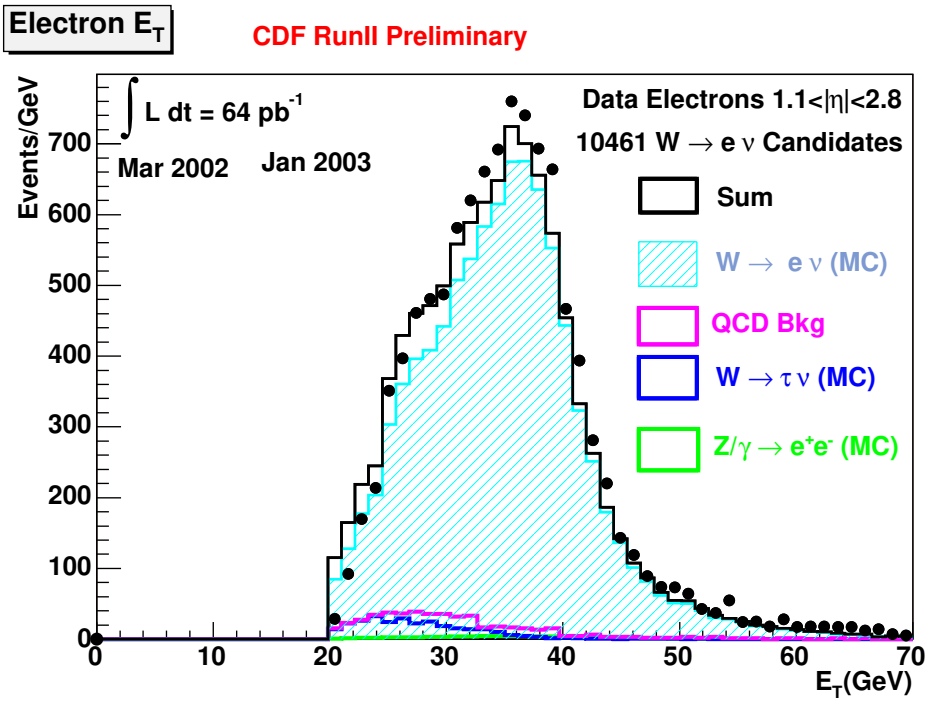

Figure 55: *E_T distribution for plug electron of W candidates compared to expected signal.*

11 Results

Various efficiencies relevant to this measurement are summarized in table 12, while table 13 is a summary of what is used for the cross section measurement. In order to correct the luminosity for the finite (±60 cm) length of the interaction region, we use the correction factor ($\epsilon_{Lum} = 0.951 \pm 0.001(\text{stat}) \pm 0.005(\text{syst})$ as estimated in previous W/Z cross section measurement [8]).

The systematic uncertainty relative to the E/P cut has been increased to 0.008 to take into account the difference in cross section we get by removing the E/P¿0.5 cut (and using only the cut E/P¡2).

	Value		Syst.error
ϵ_{Kin}	0.3112 ± 0.0007	0.0058	
$\epsilon_{Pvz,Kin}$			0.0035
ϵ_{PVZ}	0.92 ± 0.005		
ϵ_{ID}	0.961 ± 0.004		0.022
ϵ_{trig}	0.958 ± 0.011		
$\epsilon_{E/p}$	0.64 ± 0.015		0.008
ϵ		0.170 ± 0.005	0.006
$\epsilon_{tracking}$		0.322 ± 0.009	0.006
ϵ_{Lum}		0.951 ± 0.001	0.005
Overall ϵ		0.052 ± 0.002	0.002

Table 12: Efficiencies.

The value of the cross section is: $\sigma \times BR(W \rightarrow e\nu) = 2.874 \pm 0.034(stat) \pm 0.167(sys) \pm 0.172(lum)$ nb, consistent with CDF result presented in Winter 2003 and CDF results obtained in the central region.

12 Conclusion

We presented a measurement of the cross section times branching fraction for $W \rightarrow e\nu$ in CDF, where the electron is identified in the plug region by combining calori-

N.candidate events	10461	
N.background QCD events	495 ± 62 (stat)	± 247 (sys)
N.background Z events	87 ± 13 (stat)	
N.background $W \to \tau\nu$ events	324 ± 23 (stat)	
Lumin.(pb^{-1})	64	± 3.8 (sys)
ϵ	0.052 ± 0.002 (stat)	± 0.002 (sys)

Table 13: Quantities used for cross section measurement.

metric and tracking information. Tracking and calorimeter information were treated separately as in the central region. A cross section of 2.874 ± 0.240 nb is measured using 64 pb^{-1}, consistent with Run II CDF results.

Acknowledgements

We would like to thank the W/Z Cross section group, the Electroweak group and in particular Aidan Robson for useful discussions and sugggestions.

References

[1] DQM Good Run List Version 4.0 (*cf.* `http://www-cdf.fnal.gov/internal/dqm/goodrun/good.html`)

[2] Liz Sexton, private communication.

[3] C. Mills *et al* CDF Note 6108.

[4] Presentation to EWK group on 6-28-2003 by A.Robson on behalf of Young-Kee Kim, G.Manca, G.Veramendi.

[5] H.Budd, W.Sakumoto CDF Note 6433.

[6] A. Robson *et.al.* CDF Note 6642.

[7] G. Veramendi *et.al.* CDF Note 6815.

[8] W.Sakumoto, A.Hocker, CDF Note 6331.

[9] E. Halkiadakis *et al.* CDF Note 6681.

[10] W.Sakumoto, CDF Note 6341.

[11] G. Chiarelli et al. CDF Note 6864.

Appendix A: Good Run List

In the following table we list the runs that have been used for this analysis. The "Top/EWK/Exotics electron with silicon" *Good Run List Version 4.0* [1] have been used[2]

[2]With configuration (1,1,0,1).

run	Lum(Offline) pb^{-1}	$\sum$ Lum(Offline)(pb $-$ 1)
141544	0.033264	0.033264
141572	0.072336	0.105601
141576	0.094880	0.200481
141577	0.015845	0.216326
141597	0.159798	0.376124
141598	0.097837	0.473961
141618	0.103797	0.577758
141619	0.082538	0.660296
141621	0.017459	0.677754
141660	0.065542	0.743296
141984	0.089638	0.832935
142106	0.072138	0.905073
142107	0.015344	0.920417
142108	0.021320	0.941737
142109	0.014914	0.956650
142110	0.127487	1.084137
142111	0.019386	1.103523
142130	0.033327	1.136850
142131	0.036756	1.173606
142168	0.156305	1.329911
142170	0.033278	1.363189
142177	0.034471	1.397660
142202	0.181210	1.578871
144574	0.086006	1.664876
144575	0.094325	1.759201
144576	0.167405	1.926606
144578	0.056820	1.983426
144624	0.045354	2.028781
144628	0.067970	2.096750
144673	0.170547	2.267297

run	Lum(Offline) pb^{-1}	$\sum$ Lum(Offline)(pb $-$ 1)
144674	0.220514	2.487811
144694	0.112134	2.599945
144696	0.050384	2.650329
144713	0.210698	2.861027
144714	0.017673	2.878700
144883	0.052244	2.930944
144884	0.069965	3.000909
145005	0.447358	3.448267
145006	0.090170	3.538437
145032	0.068805	3.607243
145033	0.045918	3.653160
145034	0.076401	3.729561
145035	0.130984	3.860545
145036	0.049345	3.909890
145044	0.187093	4.096983
145045	0.057761	4.154744
145532	0.052674	4.207418
145608	0.168089	4.375507
145613	0.029344	4.404851
145651	0.022967	4.427818
145654	0.116387	4.544206
146850	0.013765	4.557971
146851	0.014986	4.572956
146920	0.034130	4.607087
147165	0.029123	4.636209
147804	0.110311	4.746521
147805	0.260652	5.007173
147806	0.142937	5.150110
147830	0.037038	5.187148
147832	0.057000	5.244148

run	Lum(Offline) pb^{-1}	$\sum$ Lum(Offline)(pb $-$ 1)
147834	0.052189	5.296337
147835	0.067596	5.363933
147836	0.045441	5.409375
147837	0.014659	5.424034
147843	0.014564	5.438597
147865	0.106972	5.545569
147866	0.073524	5.619093
147869	0.269089	5.888183
148153	0.094430	5.982613
148154	0.285500	6.268113
148157	0.047241	6.315353
148291	0.071657	6.387011
148293	0.262223	6.649233
148375	0.121035	6.770268
148648	0.049228	6.819496
148649	0.039382	6.858878
148674	0.093531	6.952409
148774	0.040304	6.992713
148775	0.336255	7.328968
148824	0.575499	7.904467
148825	0.016516	7.920982
148846	0.168381	8.089364
148852	0.058855	8.148219
148856	0.096198	8.244416
148857	0.175159	8.419576
148858	0.110720	8.530296
148908	0.242376	8.772672
148916	0.177514	8.950186
148950	0.080745	9.030931
148951	0.082670	9.113601

run	Lum(Offline) pb^{-1}	$\sum$ Lum(Offline)(pb $-$ 1)
148953	0.022667	9.136268
149052	0.025191	9.161459
149053	0.046369	9.207828
149055	0.052608	9.260436
149056	0.080329	9.340766
149058	0.274473	9.615239
149059	0.141696	9.756935
149264	0.161249	9.918184
149354	0.133333	10.051517
149355	0.082447	10.133964
149386	0.165363	10.299327
149387	0.567573	10.866899
149481	0.010651	10.877550
149492	0.027132	10.904682
149493	0.088920	10.993602
149663	0.273123	11.266725
149677	0.013313	11.280038
149678	0.058949	11.338986
149680	0.041489	11.380475
149681	0.023443	11.403918
149682	0.125055	11.528974
149685	0.096709	11.625683
150799	0.095982	11.721665
150801	0.037816	11.759481
150802	0.017352	11.776834
150803	0.354014	12.130847
150805	0.084695	12.215542
150819	0.035891	12.251433
150820	0.373214	12.624647
150821	0.055990	12.680637

run	Lum(Offline) pb^{-1}	$\sum$ Lum(Offline)(pb $-$ 1)
150823	0.020513	12.701150
150853	0.073745	12.774895
150856	0.185587	12.960482
150882	0.022736	12.983218
150883	0.107582	13.090800
150884	0.040159	13.130960
150885	0.253919	13.384879
150886	0.014194	13.399073
151434	0.327427	13.726500
151435	0.099237	13.825737
151436	0.060775	13.886513
151449	0.094983	13.981496
151476	0.421500	14.402996
151477	0.308585	14.711581
151509	0.020867	14.732448
151513	0.022231	14.754679
151514	0.089825	14.844503
151555	0.251322	15.095825
151556	0.142196	15.238022
151557	0.258980	15.497002
151628	0.121512	15.618513
151641	0.266933	15.885447
151683	0.158277	16.043724
151688	0.263299	16.307022
151810	0.105652	16.412674
151811	0.083949	16.496622
151841	0.052117	16.548738
151842	0.030244	16.578983
151843	0.316786	16.895769
151844	0.409480	17.305250

run	Lum(Offline) pb^{-1}	$\sum$ Lum(Offline)(pb $-$ 1)
151845	0.094817	17.400066
151868	0.078484	17.478550
151869	0.064473	17.543022
151870	0.124750	17.667772
151871	0.108020	17.775791
151872	0.081875	17.857666
151873	0.089614	17.947279
151902	0.222923	18.170202
151903	0.026383	18.196585
151906	0.038664	18.235249
151907	0.113012	18.348261
151911	0.113755	18.462015
151917	0.191397	18.653412
151918	0.056967	18.710379
151919	0.089147	18.799526
151920	0.052082	18.851608
151922	0.079267	18.930876
151971	0.329961	19.260838
151974	0.112648	19.373486
151978	0.196696	19.570183
152123	0.083222	19.653404
152124	0.030053	19.683456
152125	0.184927	19.868383
152170	0.042531	19.910915
152266	0.060241	19.971157
152267	0.113360	20.084517
152270	0.173492	20.258009
152271	0.033649	20.291658
152274	0.048718	20.340376
152459	0.133215	20.473591

run	Lum(Offline) pb^{-1}	$\sum$ Lum(Offline)(pb $-$ 1)
152464	0.139197	20.612787
152504	0.089706	20.702494
152507	0.274443	20.976936
152510	0.026414	21.003351
152514	0.098660	21.102011
152516	0.047693	21.149704
152517	0.034587	21.184290
152518	0.063948	21.248238
152520	0.307298	21.555536
152554	0.106425	21.661961
152555	0.188899	21.850859
152556	0.108257	21.959116
152559	0.049986	22.009102
152579	0.258286	22.267387
152580	0.032102	22.299490
152581	0.165645	22.465136
152582	0.091689	22.556824
152598	0.112176	22.669001
152599	0.144495	22.813496
152600	0.225683	23.039179
152601	0.078684	23.117863
152602	0.256273	23.374136
152615	0.210245	23.584381
152616	0.111693	23.696074
152617	0.259470	23.955544
152619	0.192863	24.148407
152624	0.072365	24.220772
152636	0.474341	24.695112
152639	0.043804	24.738916
152640	0.060572	24.799488

run	Lum(Offline) pb^{-1}	$\sum$ Lum(Offline)(pb $-$ 1)
152641	0.443578	25.243065
152645	0.034209	25.277273
152669	0.112757	25.390030
152674	0.118822	25.508852
152675	0.305052	25.813904
152680	0.024569	25.838472
152743	0.335144	26.173616
152745	0.101276	26.274893
152746	0.243282	26.518175
152747	0.109360	26.627535
152752	0.085422	26.712957
152772	0.121529	26.834486
152773	0.079903	26.914389
152809	0.228051	27.142439
152810	0.309517	27.451956
152811	0.038506	27.490461
152944	0.033663	27.524124
152949	0.309369	27.833494
152953	0.089671	27.923166
152954	0.173738	28.096905
152967	0.511237	28.608141
153051	0.161881	28.770021
153052	0.050980	28.821001
153054	0.734248	29.555248
153061	0.096064	29.651312
153068	0.094491	29.745804
153074	0.455962	30.201765
153075	0.409053	30.610819
153076	0.018828	30.629646
153087	0.100958	30.730604

run	Lum(Offline) pb^{-1}	$\sum$ Lum(Offline)(pb $-$ 1)
153091	0.096710	30.827314
153266	0.090338	30.917652
153268	0.100738	31.018391
153271	0.157069	31.175459
153325	0.115262	31.290720
153327	0.713073	32.003792
153343	0.177088	32.180882
153344	0.047071	32.227951
153345	0.212029	32.439980
153372	0.283785	32.723766
153373	0.025788	32.749554
153374	0.392516	33.142071
153389	1.076896	34.218967
153411	0.048908	34.267876
153412	0.297277	34.565151
153416	0.572560	35.137711
153446	0.131980	35.269691
153447	1.086472	36.356163
153460	0.012830	36.368992
153557	0.015926	36.384918
153616	0.167904	36.552822
153618	0.248599	36.801422
153620	0.056830	36.858253
153660	0.140665	36.998920
153661	0.297149	37.296070
153662	0.117767	37.413837
153693	0.270538	37.684376
153694	0.622308	38.306683
153697	0.080853	38.387535
153718	0.229803	38.617336

run	Lum(Offline) pb^{-1}	$\sum$ Lum(Offline)(pb $-$ 1)
153738	0.330028	38.947365
153739	0.255743	39.203110
154021	0.507755	39.710865
154028	0.076690	39.787556
154029	0.142860	39.930416
154030	0.276645	40.207062
154118	0.123997	40.331059
154122	0.044892	40.375950
154126	0.274832	40.650784
154175	0.334592	40.985374
154176	0.235344	41.220718
154180	0.273118	41.493835
154208	0.448710	41.942547
154449	0.114650	42.057198
154451	0.063395	42.120594
154452	0.679325	42.799919
154453	0.188865	42.988785
154518	0.249375	43.238159
154653	0.203730	43.441891
154675	0.071514	43.513405
154681	0.028408	43.541813
155113	0.573684	44.115498
155114	0.217542	44.333038
155115	0.033810	44.366848
155116	0.068275	44.435123
155121	0.022294	44.457417
155129	0.540755	44.998173
155130	0.817864	45.816036
155141	0.109787	45.925823
155145	0.093590	46.019413

run	Lum(Offline) pb^{-1}	$\sum$ Lum(Offline)(pb $-$ 1)
155146	0.123855	46.143269
155148	0.248783	46.392052
155150	0.135084	46.527134
155299	0.024650	46.551785
155301	0.083257	46.635040
155304	0.020411	46.655453
155312	0.113137	46.768589
155313	0.235639	47.004227
155318	0.060448	47.064674
155320	0.182753	47.247429
155324	0.038027	47.285458
155343	0.051345	47.336803
155344	0.058083	47.394886
155345	0.498515	47.893402
155346	0.023770	47.917171
155347	0.083827	48.000999
155364	0.584715	48.585716
155365	0.324009	48.909725
155368	0.096973	49.006699
155392	0.264464	49.271164
155743	0.117769	49.388931
155744	0.188520	49.577450
155746	0.452085	50.029533
155747	0.138378	50.167912
155763	0.048370	50.216282
155764	0.014238	50.230522
155767	0.085803	50.316326
155768	0.162317	50.478642
155770	0.389821	50.868462
155793	0.688227	51.556686

run	Lum(Offline) pb^{-1}	$\sum$ Lum(Offline)(pb $-$ 1)
155794	0.011844	51.568531
155795	0.736013	52.304543
155796	0.075718	52.380260
155818	0.241621	52.621883
155820	0.081118	52.703003
155821	0.328309	53.031311
155895	1.086951	54.118263
155918	0.601790	54.720055
155919	0.398622	55.118675
155920	0.308956	55.427631
155923	0.036043	55.463673
155996	0.349723	55.813396
155997	0.217840	56.031239
156006	0.215407	56.246647
156007	0.494619	56.741264
156081	0.454890	57.196156
156082	0.067154	57.263309
156083	0.323007	57.586315
156084	0.021990	57.608303
156087	0.016515	57.624817
156088	0.015952	57.640770
156089	0.318921	57.959690
156098	0.230231	58.189922
156100	0.376377	58.566299
156103	0.371151	58.937450
156112	0.028567	58.966019
156116	0.990868	59.956886
156117	0.194400	60.151287
156118	0.194771	60.346058
156369	0.291782	60.637840

run	Lum(Offline) pb^{-1}	$\sum$ Lum(Offline)(pb $-$ 1)
156372	0.028260	60.666100
156401	0.064980	60.731079
156452	0.034189	60.765266
156454	0.043765	60.809032
156455	0.086483	60.895515
156457	0.084387	60.979900
156458	0.131713	61.111614
156460	0.385088	61.496704
156464	0.051504	61.548210
156484	1.046637	62.594849
156487	0.121033	62.715881

Table 14: Good Run List version 4.0 used for this analysis. The overall 1.019 correction factor for luminosity has to be applied.